AD NUMBER
AD363573
CLASSIFICATION CHANGES
TO: **UNCLASSIFIED**
FROM: **CONFIDENTIAL**
LIMITATION CHANGES
TO: **Approved for public release; distribution is unlimited.**
FROM: **Distribution authorized to DoD only; Administrative/Operational Use; MAR 1953. Other requests shall be referred to the Defense Nuclear Agency, Washington, DC. Pre-dates formal DoD distribution statements. Treat as DoD only. Formerly Restricted Data.**
AUTHORITY
DNA/SSTL ltr dtd 19 Oct 1995 and (DSWA/OPSSI) ltr dtd 11 Jun 1997 DNA/SSTL ltr dtd 19 Oct 1995 and (DSWA/OPSSI) ltr dtd 11 Jun 1997

AD# 363573

SECURITY MARKING

The classified or limited status of this report applies to each page, unless otherwise marked.
Separate page printouts MUST be marked accordingly.

"This document contains information affecting the National Defense of the United States within the meaning of the Espionage Laws, Title 18, U. S. C., Section 793 and 794. Its transmission or the revelation of its contents in any manner to an unauthorized person is prohibited by law."

EXCLUDED FROM AUTOMATIC
REGRADING; DOD DIR 5200.10
DOES NOT APPLY

DISCLAIMER NOTICE

THIS DOCUMENT IS BEST QUALITY AVAILABLE. THE COPY FURNISHED TO DTIC CONTAINED A SIGNIFICANT NUMBER OF PAGES WHICH DO NOT REPRODUCE LEGIBLY.

[redacted]

[redacted] EC

(19) WT-613

This document consists of 55 pages
No. 272 of 280 copies, Series A

Report to the Scientific Director

(6) PEAK OVERPRESSURE VS DISTANCE IN FREE AIR [U]. KS

(10) By

J. F. Moulton, and P. Hanlon,

U. S. Mil... FROM ... DIRECTLY ... Sponsoring Agency to.

(5) Naval Ordnance Laboratory, White Oak, [redacted] Md.

(11) Mar...

[redacted]

[redacted]

ABSTRACT

At the request of the Height of Burst Panel, Project 6.13 was organized to make measurements on King Shot, Operation Ivy, that would establish the peak shock overpressure in the blast wave as a function of distance from the burst in the free-air region. This information was required in particular to determine whether scaling laws could be used with existing data obtained on Operation Tumbler to predict free-air pressures from much larger weapons. Secondary objectives were to record and determine the magnitude of a precursor wave or other visibly observable thermal effects that might occur and to collect any additional information that might explain the departure of the free-air blast measurements obtained on Operation Greenhouse from the Operation Tumbler composite free-air pressure results. (The four free-air pressure-distance curves obtained on Operation Tumbler scaled very well over the entire pressure range measured. The composite result is considered to be highly reliable.)

Data were collected using the photo-optical technique more frequently referred to as "rocket smoke-trail photography." This technique has been built around the shock-velocity method of peak-blast-pressure determination.

The results obtained can be summarized as follows:

For the fireball region the equation which was fitted to the radius-time data is

$$R\ (\text{ft}) = 3302.3t^{0.366}\ (\text{sec}) \qquad R \leq 900\ \text{ft}$$

The shock overpressure in this region is related to distance by

$$P\ (\text{psi}) \propto R^{-4.32}\ (\text{ft}) \qquad R \leq 900\ \text{ft}$$

For the free-air region the equation that was fitted to the arrival-time data by the method of least squares is

$$t\ (\text{sec}) = 0.00141\left(R - \int_{R_0}^{R} \frac{5056.6^{1.6}}{5056.6^{1.6} + R^{1.6}}\,dR\right) - 0.6238$$

for values of the radial distance R between [redacted] distance and shock velocity U in feet per second is

$$U = 707.6\left[1 + \left(\frac{5056.6}{R}\right)^{1.6}\right] \qquad 900\ \text{ft} \leq R \leq 3250\ \text{ft}$$

The radiochemical kilotonnage equivalent, based on a comparison of the King Shot results with the Operation Tumbler composite results, is 541 ± 30 kt. The TNT efficiency of King Shot was found to be 38.8 ± 2.0 per cent within the pressure range of 200 to 80 psi.

[redacted]

The precursor wave detected over the land area by pressure-time gauges of Project 6.1 (WT-602) was not observed in the motion-picture films exposed particularly for Project 6.13. Palm trees on an island in the foreground obscured the island nearest the burst, where the precursor wave was detected. No precursor was observed over the water either by gauges or photographically. No positive evidence was found to explain the departure of Operation Greenhouse free-air measurements from the Tumbler composite free-air pressure results.

[redacted]

[redacted]

[redacted]

ACKNOWLEDGMENTS

C. L. Karmel and LT B. M. Loring, USNR, both of the U. S. Naval Ordnance Laboratory (NOL), aided immeasurably in the successful completion of the preparatory, field, and data-analysis phases of Project 8.13. Their timely suggestions and attention to detail simplified the total effort considerably.

Grateful appreciation is expressed for the successful photographic records obtained by the staff of Edgerton, Germeshausen & Grier, Inc. The excellent cooperation received in this operation, as in previous ones, is indeed commendable.

Appreciation is expressed to CDR J. H. Lofland, USN, of the Armed Forces Special Weapons Project; E. F. Cox, of the Sandia Corporation; and F. B. Porzel, of the Los Alamos Scientific Laboratory, for their guidance and assistance on various administrative and technical phases of this project.

H. P. Feldman, of the NOL, redesigned the rocket-launching equipment to produce the novel fan-type optical grid used in the experiment.

T. S. Walton, of the NOL, deserves much credit for his work on the IBM mechanization of the data-reduction phase of record analysis. The procedure that he developed effectively reduced the time required to complete this phase by 65 per cent, compared with previous analyses.

[redacted]

[redacted]

CONTENTS

[redacted]

CONTENTS (Continued)

ILLUSTRATIONS

CHAPTER 2 INSTRUMENTATION

CHAPTER 3 RESULTS

CHAPTER 4 ANALYSIS AND DISCUSSION OF RESULTS

TABLES

CHAPTER 1

INTRODUCTION

1.1 OBJECTIVES

Upon the recommendation of the Height of Burst Panel, the U. S. Naval Ordnance Laboratory (NOL) was requested by the Armed Forces Special Weapons Project (AFSWP) to participate in King Shot, Operation Ivy. In particular, the NOL was asked to conduct the necessary experiments required to obtain the following information:

1. Peak shock overpressure as a function of distance in the free-air region. This information was required in particular to determine whether scaling laws could be used with existing data obtained on Operation Tumbler to predict free-air pressures from much larger weapons.

2. Information relative to the formation and magnitude of any precursor wave or other visibly observable thermal effect.

3. Additional information that might explain the departure of the free-air measurements obtained on Operation Greenhouse from the Operation Tumbler composite free-air pressure results. (The four free-air pressure-distance curves obtained on Operation Tumbler scaled very well over the entire pressure range measured. The composite result is considered to be highly reliable.)

1.2 HISTORY

In order to obtain the desired information required by objective 1, the photo-optical technique, which is now known as the "rocket smoke-trail photography method," seemed to be adequate with only a slight modification. This technique was developed at the NOL for use in Operation Greenhouse where it proved to be quite successful.[1] Highly satisfactory results were also obtained later on Operations Jangle[2] and Tumbler.[3]

On the fourth shot of the Tumbler series of tests, a precursor wave appeared in the rocket smoke-trail films and was analyzed quantitatively for the first time. (Such waves also appeared in certain films of Operation Buster, in which the NOL did not participate, but were not analyzed at the time.) Thus it was believed that, in the same experiment designed principally to accomplish objective 1, the information sought in objective 2 would be obtained.

With regard to the last objective the rocket smoke-trail method used in the four shots of Operation Tumbler yielded such consistent measurements after the application of scaling laws that a highly reliable pressure-distance curve was made available. Comparison of Tumbler and Greenhouse free-air data[3] showed that the pressures observed on Greenhouse were increasingly higher than those obtained on Tumbler as the equivalent reduced distance from the bomb increased. Repeated checking of all the data not ated the possibility of error in the Greenhouse calculations, and it was shown conclusively that the arrival times observed on

Operation Greenhouse led to higher shock velocities, and hence higher pressures, at equivalent scaled distances.

On Operation Ivy it was hoped that some information might be gained to solve this problem. Tests on Operation Tumbler were conducted at the AEC Nevada Proving Grounds (NPG) at an altitude of approximately 4000 ft above sea level, whereas Operation Greenhouse took place at Eniwetok Atoll in the Marshall Islands, virtually at sea level. The atmosphere at the NPG was dry, whereas the island site was comparatively moist and humid. It was thought that possibly the cause of the disagreement might stem from these atmospheric differences or from the fact that the Greenhouse tests were tower shots whereas those of Tumbler were airdrops.

During the planning phase it was announced that King Shot, Operation Ivy, was to be an airdrop similar to those on Tumbler but at the island site. This presented an excellent opportunity to resolve the difficulty at least partially, if indeed such environmental conditions were the cause of the disagreement.

1.3 OPERATIONS

Project 6.13 was organized in two groups, one which went into the field and one which aided in the pretest preparations and posttest analysis at the NOL. Administrative details within the project were carried out jointly by J. F. Moulton, Jr., and P. Hanlon. E. F. Cox and F. B. Porzel were the directors of Program 6 and provided over-all supervision and technical guidance.

Project 6.13 personnel included J. F. Moulton, Jr., Project Officer, Analysis; the field party composed of P. Hanlon, Field Project Officer, Analysis; B. M. Loring, Supply and Analysis; and C. L. Karmel, Instrumentation and Analysis; and J. R. Mitchell, Supply Officer. In the field, Karmel, as the assistant to the Field Project Officer, was largely responsible for instrumentation. Loring served as Supply Officer in the field and assisted in the installation of equipment. Labor was provided by Holmes & Narver through Task Group (TG) 132.1.

1.4 BACKGROUND: DETERMINATION OF PEAK SHOT OVERPRESSURE BY THE VELOCITY METHOD

The photo-optical technique used on King Shot, Operation Ivy, to obtain arrival-time data for the determination of peak shock overpressures is explained in detail in reports on Operations Greenhouse[1] and Jangle.[2] Briefly the technique consisted in establishing a rocket smoke-trail grid behind the burst and recording the shock-wave growth as a function of time with high-speed motion-picture cameras. The position of the shock front is determined by recording photographically the light rays reflected from the grid; those rays which pass tangentially to the shock front are refracted, causing breaks to appear in the otherwise continuous grid lines. With the explosion center as zero, frame-by-frame measurements of the distance are made on 20× magnified images in a direct-projection Recordak. Time per frame is also noted.

From these arrival-time data the instantaneous shock velocity at known distances can be determined. This is best done by fitting the data with a smooth curve which can be expressed in closed mathematical form. Differentiation of the equation yields an expression for the velocity as a function of radial distance from the burst.

In the early stages, i.e., the fireball region, an exponential function is used

$$R = Kt^n \tag{1.1}$$

where R = distance from weapon zero
t = time
K = constant
n = the slope of the log-log plot of R and t

[redacted]

Differentiation of this equation gives

$$U = nKt^{n-1} \tag{1.2}$$

where U is the instantaneous shock velocity.

On prior tests the free-air arrival-time data were fitted by a cubic polynomial by the method of least squares. On this te new fitting function is introduced. The new equation is

$$t = \frac{R}{a} - \frac{1}{a}\int_{R_0}^{R} \frac{b^{1.8}}{b^{1.8} + R^{1.8}}\, dR + C \tag{1.3}$$

where a, b, and C are constants. At first glance this equation appears clumsy, but it is readily fitted by the method of least squares to the arrival-time data on IBM equipment. The advantages of the use of the new equation are twofold: (1) A more realistic approach to the solution of the problem is made in view of the physical nature of the phenomenon, and (2) considerable time is saved in the analysis of this type of data. Upon differentiation, a comparatively simple function results:

$$U = a\left[1 + \left(\frac{b}{R}\right)^{1.8}\right] \tag{1.4}$$

Fitting the King Shot data by both the new form and the polynomial used previously led to identical pressure results. (A comparison of the instantaneous shock velocities, which is an extremely critical comparison, indicated that agreement between the two sets of results was within ±0.36 per cent over the entire range.) Some of the Tumbler data have been fitted using the new form, and a comparison showed the pressure results of both methods to be identical. A full explanation of the derivation of the equation and the method of fitting data by the new function are given in the Appendix.

The peak pressure in the shock wave is a known function of the velocity and can be calculated using the Rankine-Hugoniot relation:*

$$P_s = \frac{2\gamma P_0}{\gamma + 1}\left[\left(\frac{U}{C_0}\right)^2 - 1\right] \tag{1.5}$$

where P_s = peak shock overpressure (psi)
P_0 = ambient pressure ahead of the shock (psi)
γ = the ratio of specific heats for air, 1.40
C_0 = speed of sound ahead of shock (ft/sec)
U = instantaneous shock velocity (ft/sec)

P_0 and T_0 are measured directly, and

*In regions of very high pressure the Rankine-Hugoniot relation, as written, is in error because the equation of state on which it is based no longer applies. Furthermore, the ratio of specific heats for air (γ) becomes meaningless. To overcome the difficulties introduced by these variations, corrections are made by use of the Hirschfelder-Curtiss tables[4] which give P_s in terms of U, the changes in γ and the equation of state being taken into account (see also Sec. 3.5).

[redacted]

$$C_s = 1088\sqrt{1 + \frac{T_c}{273}} \qquad (1.6)$$

where T_c is the ambient temperature in degrees centigrade and C_s is the velocity of sound in feet per second

REFERENCES

1. J. F. Moulton, Jr., and B. T. Simonds, Peak Pressure vs Distance in the Free-air and Mach Regions Using Smoke-rocket Photography, Greenhouse Report, Annex 1.6, Part II, Sec. 1, WT-54.
2. J. F. Moulton, Jr., E. R. Walthall, and P. Manion, Peak Pressure vs Distance in Free Air Using Smoke Rocket Photography, Buster-Jangle Project 1.3b Report, WT-389.
3. C. J. Aronson, J. F. Moulton, Jr., et al., Free Air and Ground Level Pressure Measurements, Tumbler-Snapper Projects 1.3 and 1.5 Report, WT-813.
4. J. O. Hirschfelder and C. F. Curtiss, Thermodynamic Properties of Air, Vol. II, University of Wisconsin (NRL), Dec. 31, 1946.

CHAPTER 2

INSTRUMENTATION

A plan view of the Project 6.13 instrumentation layout is shown in Fig. 2.1.

2.1 ROCKET SMOKE-TRAIL DETECTION GRID

2.1.1 Smoke Rockets

To establish the shock-wave detection grid, 19 smoke-producing rockets were fired 7 sec prior to burst time from Station 6140. Each round was a modified 5"0 Rocket Head Mark 10 with a 5"0 Spin Stabilized Motor Mark 3. Ten pounds of FS chemical smoke mix was released from each head during its upward trajectory. The smoke rocket, as used on this and previous operations, was developed for this purpose at the NOL[1] in 1950.

2.1.2 Rocket Launchers

On previous operations the smoke trails were established in the form of a vertical-line grid. This form was not feasible in the Ivy test because of limited dry land areas on which to locate rocket launchers. In its place a fan-type grid was used, as was first suggested by C. J. Aronson of the NOL (see Fig. 2.2). The rocket launchers,[1] in two identical batteries facing in opposite directions, were aligned so that the direction of fire was perpendicular to the line of sight of the cameras (Figs. 2.1 and 2.3). Each battery consisted of nine launchers with elevation angles of 10, 20, 30, 40, 50, 60, 70, 80, and 85°. At one end of the launching plot, a single launcher, at 60° elevation, was arranged to fire parallel to the line of sight (Figs. 2.4 and 2.5).

2.1.3 Power and Timing

Considerable saving in construction and labor costs was effected through the use of a novel power-and-timing station. Timing relays, time-delay devices, and power take-off switches were mounted inside a waterproofed wooden box the size of a standard foot locker. Before evacuation the necessary switches were closed in the ready position, and the box was sealed and buried beneath sandbags. The station proved to be just as satisfactory as the reinforced-concrete blast shelters costing several thousands of dollars that were used in previous operations.

The circuitry and all other details concerning the establishment of the rocket smoke-trail grid are given in reference 2.

2.2 PHOTOGRAPHIC INSTRUMENTATION

The photographic records for Project 6.13 were obtained by the staff of Edgerton, Germeshausen & Grier, Inc. (EG&G). Three high-speed Mitchell cameras were installed in

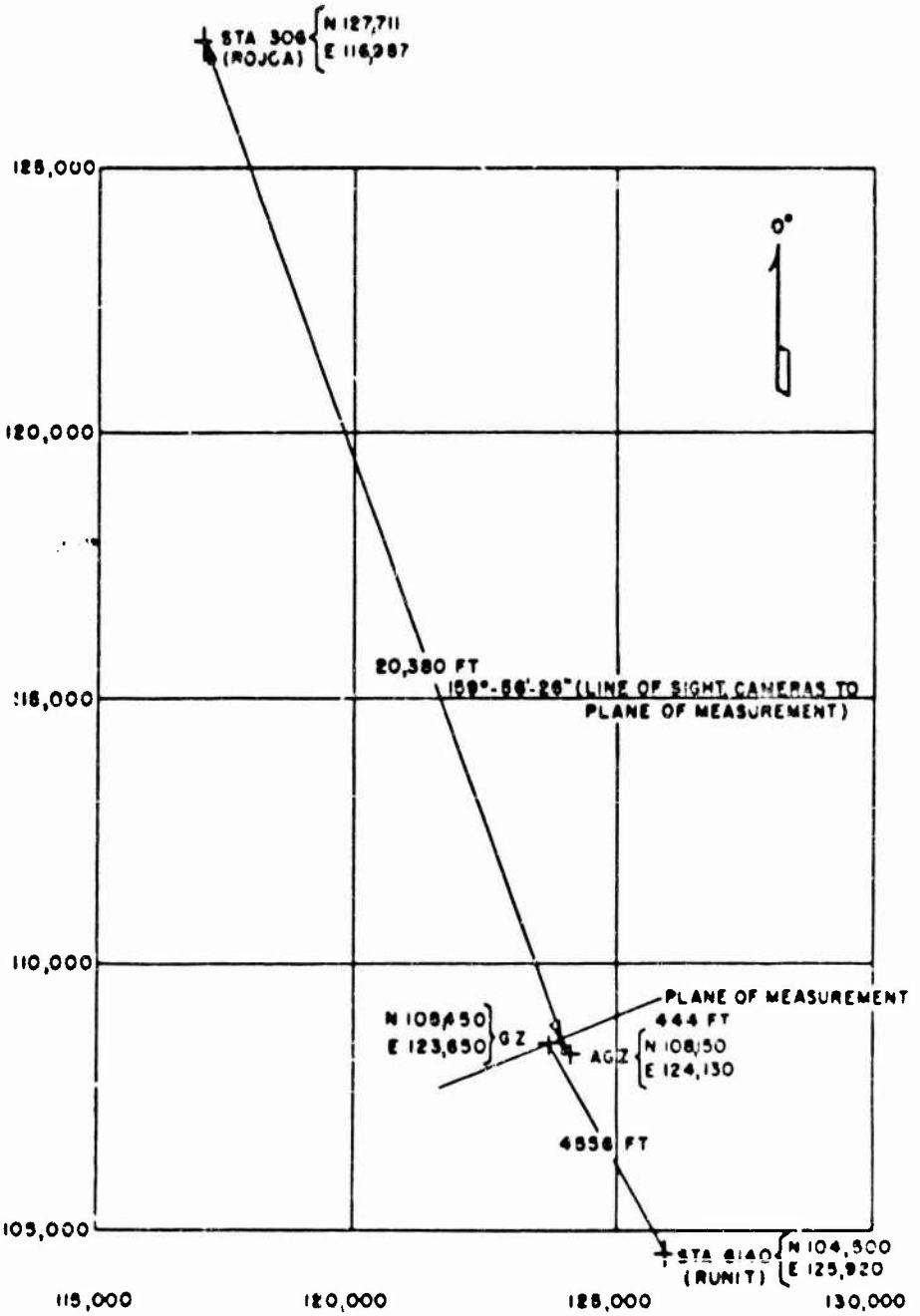

Fig. 2.1 — Test layout, Project 6.13, showing plane of measurement.

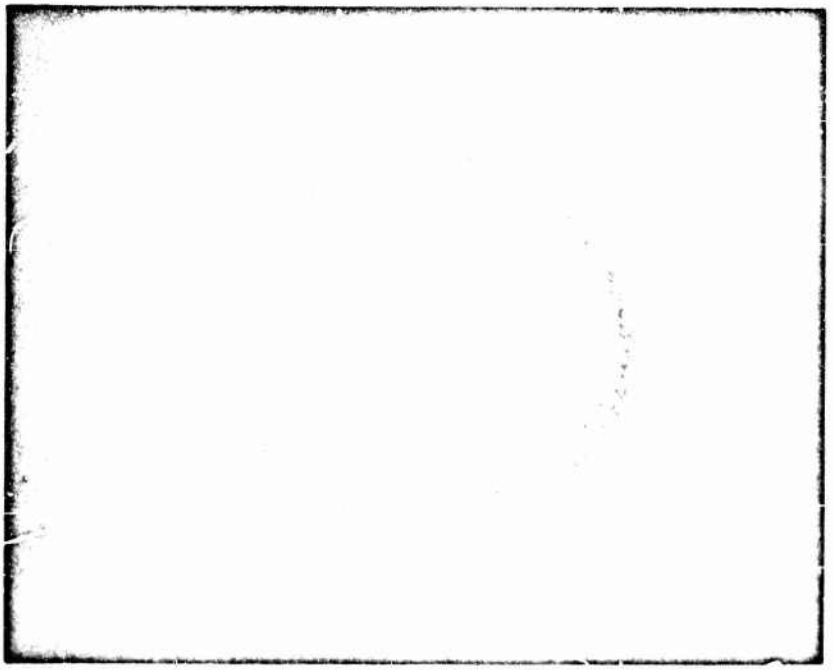

Fig. 2.2—The smoke-rocket fan grid at 0.0228 sec.

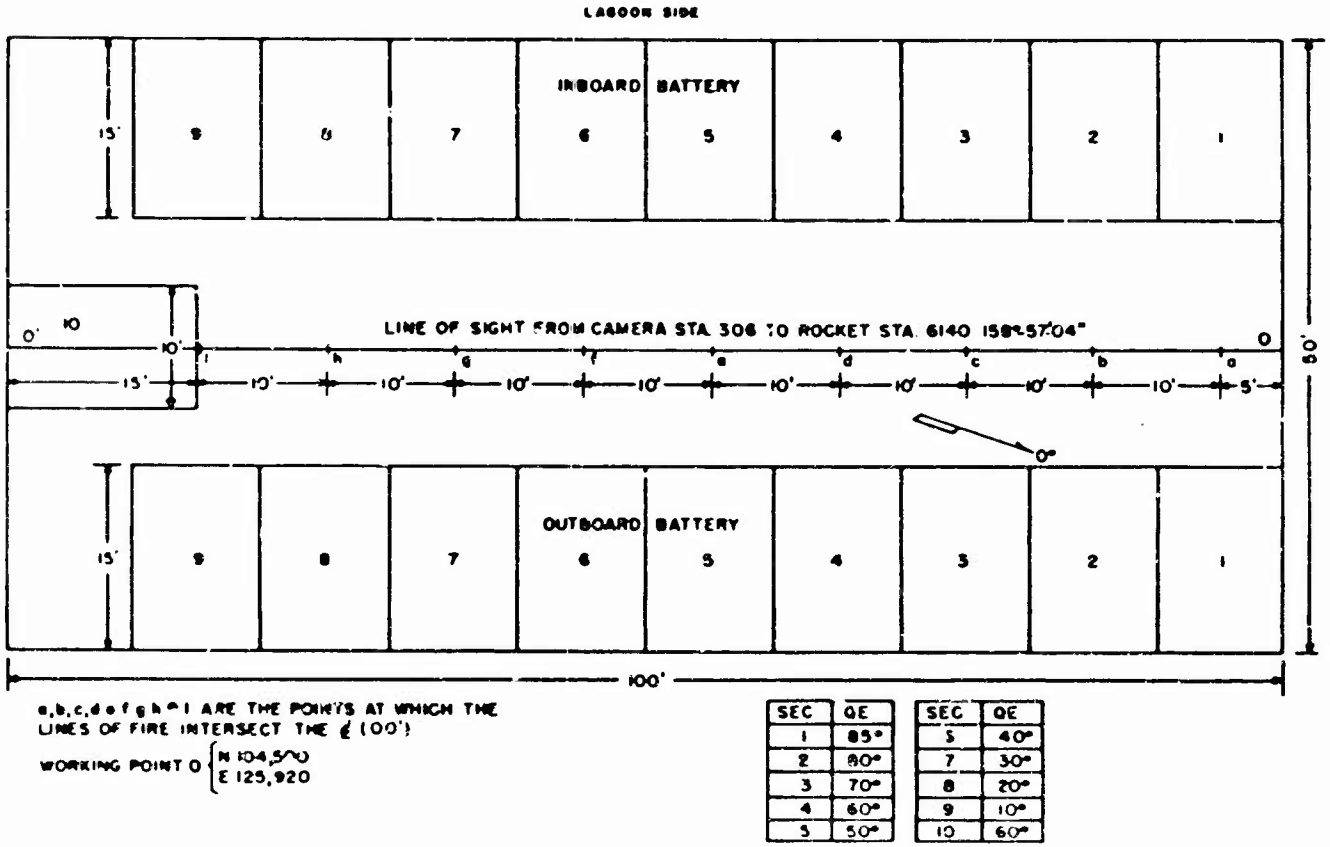

SEC	QE
1	85°
2	80°
3	70°
4	60°
5	50°

SEC	QE
5	40°
7	30°
8	20°
9	10°
10	60°

Fig. 2.3—Plan view of NOL Rocket Station 6140.

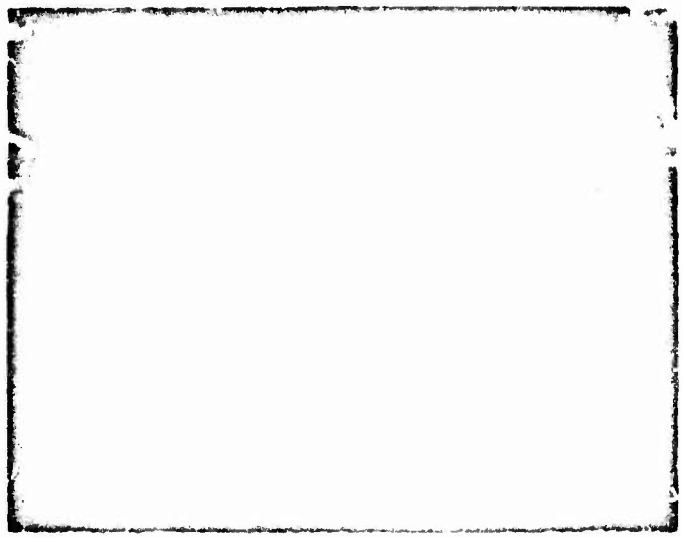

Fig. 2.4—NOL rocket launchers, Station 6140.

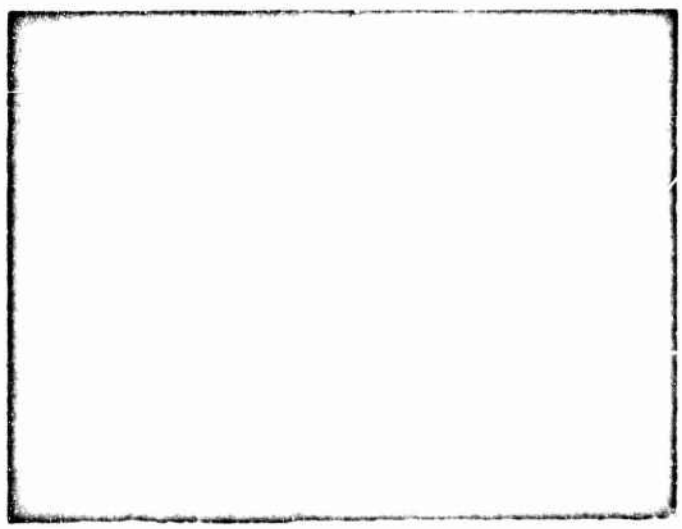

Fig. 2.5—Outboard smoke-rocket battery, Station 6140.

Station 306 for the specific use of this project, but one of them failed to function. Complete photographic details are given in Table 2.1

The use of fiducial markers was unnecessary on this test. The base line of the plane of measurement was readily established by utilizing the horizon. On Operation Tumbler[3] it was determined that all that is required for distance calibration is an accurate calibration "rose" placed on the film before processing, the accurately measured focal length of the lens used, and the range to the desired objective plane. Vertical and horizontal scales can be established with an accuracy of better than 0.01 per cent in this fashion.

Timing marks were placed on the film during the recording period at the rate of 1.96 cps. This very low rate is discussed further in Secs. 3.3 and 3.7.2.

Table 2.1 — PHOTOGRAPHIC DETAILS

Film No.	16293	16291
Station	306	306
Camera	MMH-1	MMH-7
Effective aperture	f/11-15°	f/11-15°
Effective focal length, mm	99.98	35.28
Nominal frame rate, frames/sec	85	80
Timing marks, cps	1.96	1.96
Vertical aiming	4° 08′	4° 08′
Horizontal aiming	GZ*	GZ*

*Ground zero.

REFERENCES

1. J. F. Moulton, Jr. and B. T. Simonds, An FS Smoke Target Rocket (5"/ Spinner Type), U. S. Naval Ordnance Laboratory Report NavOrd 1571, October 1950.
2. J. F. Moulton, Jr., and B. T. Simonds, Peak Pressure vs Distance in the Free-air and Mach Regions Using Smoke-rocket Photography, Greenhouse Report, Annex 1.6, Part II, Sec. 1, WT-54.
3. C. J. Aronson, J. F. Moulton, Jr., et al., Free Air and Ground Level Pressure Measurements, Tumbler-Snapper Projects 1.3 and 1.5 Report, WT-513.

CHAPTER 3

RESULTS

3.1 INSTRUMENTATION AND RECORDS

The rocket smoke-trail fan grid was established just prior to zero time and was satisfactory in most respects. As can be seen in Fig. 2.2, the grid appeared to be somewhat lacking in contrast in the upper right-hand portion of the object plane, but this did not interfere seriously with measurements made on the film originals. If the smoke trails had been approximately 1000 ft closer to the burst, they would have appeared in greater contrast but possibly would have been in the region where trail evaporation occurs. The grid was placed at the distance chosen so that, if the atmosphere were clear (greater than 98 per cent transmission), good contrast could be expected.

Of the three cameras assigned specifically to Project 6.13, only two functioned properly. The camera having a 50-mm focal-length lens failed to operate. Records were obtained by the cameras having lenses of 100- and 35-mm focal length; however, only the record from the camera equipped with the 100-mm focal-length lens was used for the analysis. The other record, which should have been of greater value from the standpoint of larger usable field of view, proved to be of little additional quantitative value because of the poor atmospheric conditions that existed. The high humidity led to such low contrast that the rocket smoke trails were not visible much farther away from the center of burst on the 35-mm film with a wider field of view than on the longer-focal-length record. This condition, coupled with poorer space resolution, made the short-focal-length record of qualitative value only.

3.2 TIME AND DISTANCE SCALES

The arrival-time data for King Shot were measured from film 16293. The vertical plane of measurement is shown in Fig. 2.1. The timing marks placed on the film at the rate of 1.98 cps were not sufficient by themselves to ascertain whether the film speed was constant during the period of interest. However, from additional information available it was determined that in all probability the film speed was constant. The time per frame was found to be 0.011754 ± 0.000150 sec (the last two decimal places were held for computational reasons). Timing accuracy is discussed in detail in Sec. 3.7.2.

The distance scale for both horizontal and vertical measurements was found to be 10.686 ft/mm on the enlarged image. Thus measurements made to 0.1 mm with relative ease were far better than the maximum static resolution uncertainty of ±6 ft. Accuracy considerations are developed further in Sec. 3.7.3.

3.3 ARRIVAL TIME DATA

Arrival-time data were obtained over the ranges 600 to 3250 ft in distance and 0.0 to 0.7 sec in time. These data are given in Table 3.1 and are plotted in Fig. 3.1 together with the

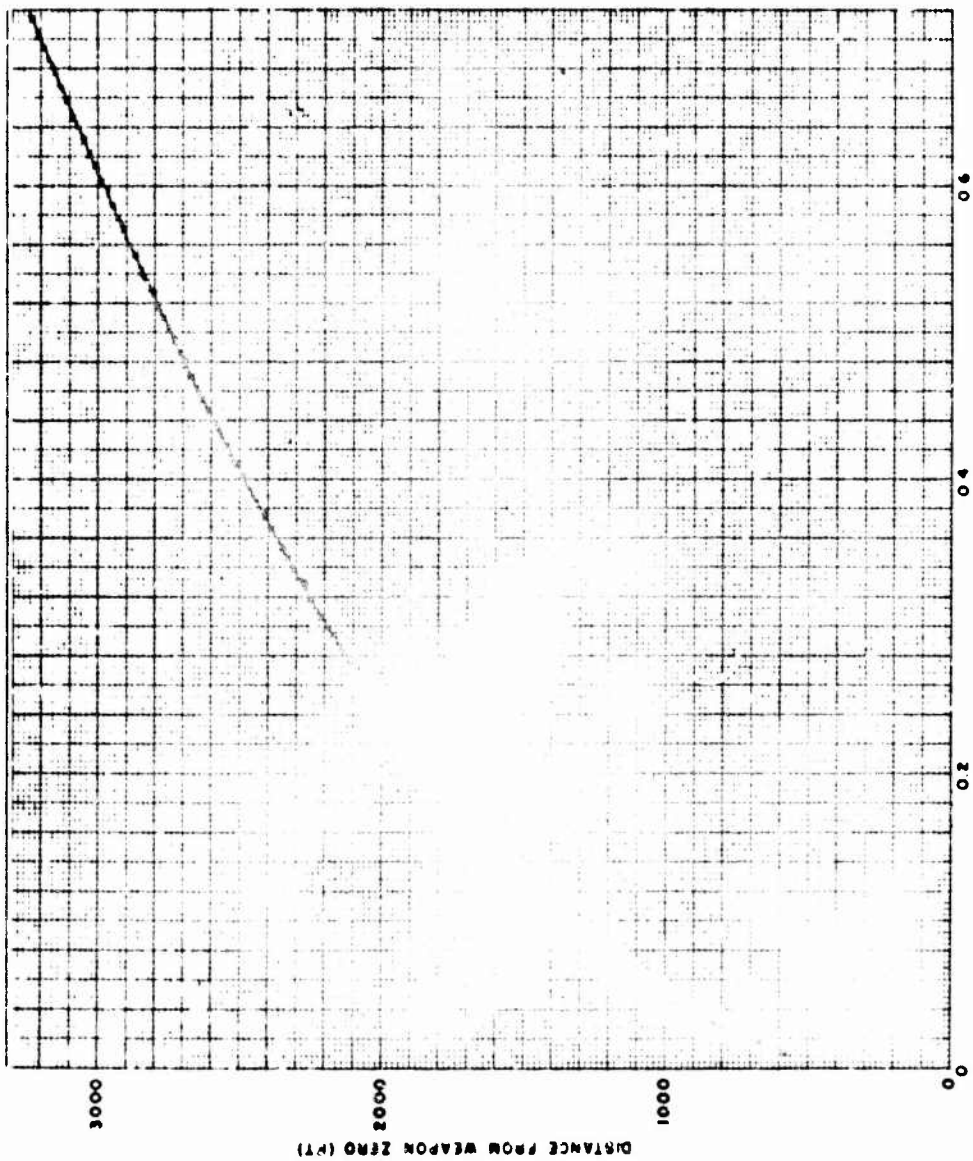

Fig. 3.1 — Arrival-time curve, King Shot.

curve fitted to the data by the method of least squares. As can be seen, the scatter in the data is small.

Table 3.1 — ARRIVAL-TIME DATA*†

Distance from weapon zero, ft	Arrival time, sec	Distance from weapon zero, ft	Arrival time, sec	Distance from weapon zero, ft	Arrival time, sec
580.923	0.011320	2023.469	0.245400	2699.618	0.481480
781.318	0.023074	2048.872	0.258154	2732.080	0.493234
897.800	0.034828	2089.885	0.289908	2749.578	0.504986
1000.087	0.046582	2137.941	0.281662	2791.122	0.516742
1094.793	0.058338	2183.091	0.293416	2804.514	0.528496
1175.607	0.070090	2203.964	0.305170	2845.958	0.540250
1251.078	0.081844	2244.839	0.318924	2866.850	0.552004
1320.138	0.093598	2287.949	0.328878	2900.026	0.563758
...	...	2316.205	0.340432	2921.398	0.5755'2
1469.712	0.117106	2345.628	0.352186	2942.334	0.587266
1528.054	0.126860	2385.539	0.363940	2974.888	0.599020
1578.978	0.140614	2418.928	0.375694	3003.588	0.610774
1633.078	0.152368	2443.006	0.387448	3037.651	0.622528
1680.685	0.164122	2485.919	0.399202	3058.324	0.634282
1744.082	0.175878	2523.489	0.410958	3092.487	0.646036
1799.049	0.187830	2549.805	0.422710	3112.091	0.657790
1842.262	0.199384	2580.963	0.434464	3145.186	0.669544
1878.989	0.211138	2611.152	0.446218	3182.084	0.681298
1919.371	0.222892	2643.579	0.457972	...	...
1959.378	0.234648	2682.018	0.489726	3212.146	0.704806
				3240.298	0.716560

*All decimal places in distances and the last two decimal places in times are held for computational reasons only.

†The zero times on the rocket trail films were established by preliminary fireball data measured at the Test Site. Later and more complete measurements have resulted in radius-time curve changes which give an error of 0.25 msec in the absolute time of the radius-time curves shown here. Because of the scaling methods, this absolute error does not affect the validity of the pressure-distance curve or the scaled yield.

3.3.1 Fireball Region

In the early stages of shock growth, i.e., the fireball region, the radius increased exponentially with time, and the data form a straight line when plotted on a log-log graph as in

Fig. 3.2. The curve fitted to these data is

$$R = 3302.3t^{0.388} \qquad 600 \text{ ft} \le R \le 900 \text{ ft} \tag{3.1}$$

where R is the distance from weapon zero in feet and t is the time in seconds. The fireball measurements made on the rocket-smoke-trail photographs are in excellent agreement with those made by EG&G on the high-speed-camera records of considerably better time resolution. As discussed in Sec 3.7.2, this fact was used in the timing-accuracy determination.

3.3.2 Free-air Region

Over the latter portion of the arrival-time curve, the data were fitted by

$$t = 0.00141\left(R - \int_{R_0}^{R} \frac{5056.6^{1.5}}{5056.6^{1.5} + R^{1.5}}\,dR\right) - 0.6236 \tag{3.2}$$

where R is the radial distance from weapon zero over the range 900 ft ≤ R ≤ 3250 ft.

Measurements of the first few frames of the film record showed that the fireball growth was symmetrical about the burst point. Shortly after shock breakaway, a few frames indicated that the shock wave out to about 1300 ft was also symmetrical about the center of the burst, but, in the latter three-fourths of the record, only the eastern side of the fan grid was visible. As a result it cannot be said with certainty that the shock wave was symmetrical over this region.

3.4 METEOROLOGICAL DATA

The atmospheric pressure P_0 and temperature T_0 were measured prior to the shot. The data from both surface and upper-air observations were used. The velocity of sound C_0 at the various levels was computed using Eq. 1.6.

Both P_0 and C_0, for lack of more complete data, were assumed to vary linearly with altitude. These data are given in Table 3.3 and plotted in Fig. 3.3.

Table 3.3 — METEOROLOGICAL DATA

Altitude, ft	Pressure, psi	Temperature, °C	Velocity of sound, ft/sec
0	14.649	28.8	1143.9
310	14.504	28.5	1143.5
1460*	13.96*	25.4*	1138.1*
2390	13.632	23.3	1135.9

*Interpolated from Radiosonde data.

3.5 PEAK-SHOCK-OVERPRESSURE–DISTANCE DATA

Equations 3.1 and 3.2 were differentiated to obtain expressions for the instantaneous shock velocities, U, at desired distances. For the fireball region

$$U = 1281\,R^{-0.613} \qquad 600 \text{ ft} \le R \le 900 \text{ ft} \tag{3.3}$$

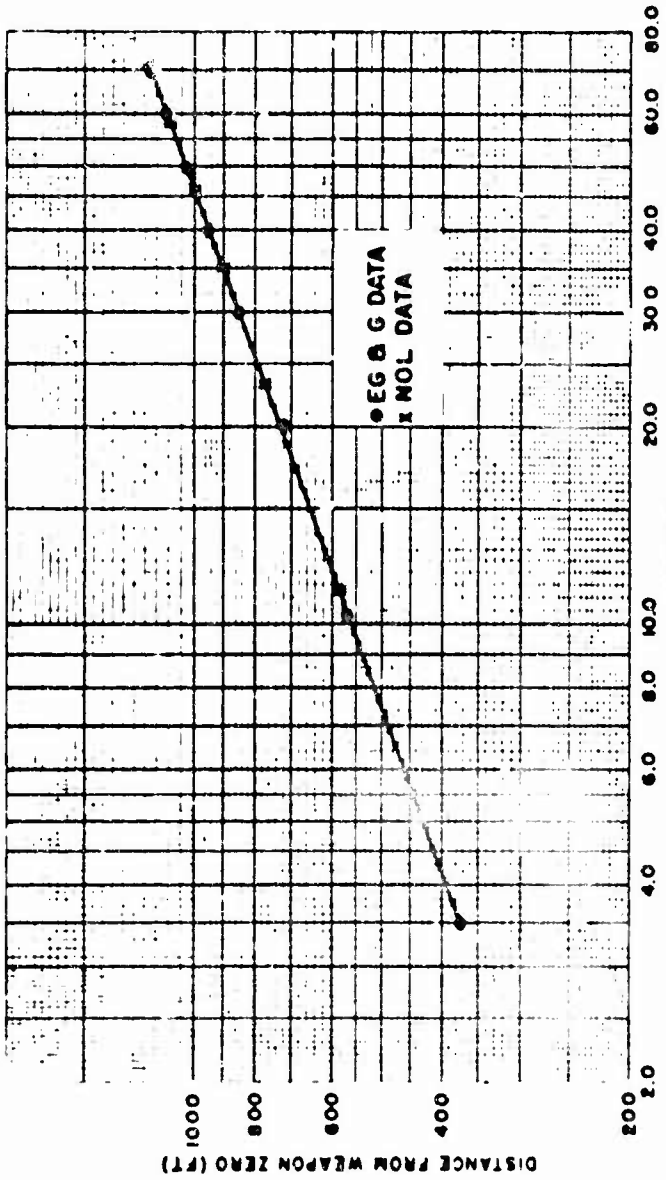

Fig. 3.2—Fireball radius vs time, NOL and EG&G data.

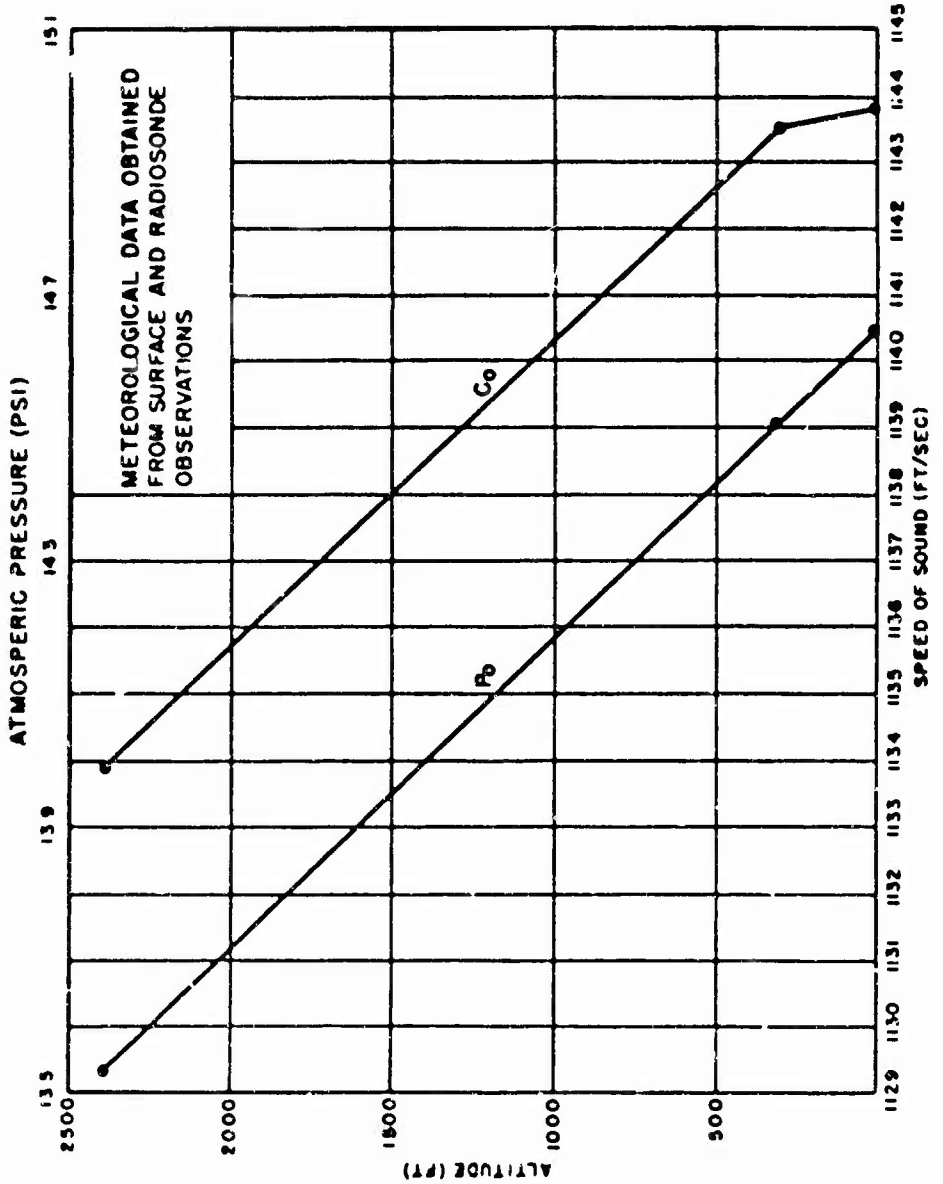

Fig. 3.3—Atomospheric pressure (P_o) and speed of sound (C_o) vs altitude.

is obtained. This result leads to the relation

$$P \propto R^{-3.33} \tag{3.4}$$

which is in effective agreement with theory.* For the free-air region

$$U = 707.5\left[1 + \left(\frac{5056.6}{R}\right)^{1.6}\right] \qquad 900 \text{ ft} \le R \le 3250 \text{ ft} \tag{3.5}$$

These values, together with the corresponding meteorological data from Fig. 3.3, were used to enter the Hirschfelder-Curtiss tables[1] from which the peak shock overpressures were obtained for the corresponding distances. The values are given in Table 3.3 and plotted in Fig. 3.4. For pressures below approximately 100 psi the values from the Hirschfelder-Curtiss tables agree exactly with those that would be obtained using the Rankine-Hugoniot pressure-velocity relation, Eq. 1.5. Above the 100-psi level, variations in γ and the equation of state, on which the Rankine-Hugoniot relation depends, begin to take significant effect. These variations are accounted for in the Hirschfelder-Curtiss tables. For these reasons values from these tables have been used throughout the calculations.

Table 3.3 — PEAK-OVERPRESSURE-DISTANCE DATA

Distance from weapon zero, ft	Peak overpressure, psi	Distance from weapon zero, ft	Peak overpressure, psi	Distance from weapon zero, ft	Peak overpressure, psi
600	4830	1500	341	2400	92.0
700	2959	1600	291	2500	82.6
800	1932	1700	238	2600	74.6
900	1381	1800	203	2700	67.3
1000	1016	1900	172	2800	60.0
1100	782	2000	151	2900	54.8
1200	613	2100	132	3000	49.7
1300	496	2200	116	3100	45.3
1400	405	2300	102	3200	41.0

A word about the use of the meteorological data in carrying out the pressure calculations is in order. For the sake of uniformity with other air blast data[2] published previously, the values of P_0 and C_0 were taken along a vertical line from weapon zero to ground zero (GZ) at distances corresponding to those selected for substitution in the shock-velocity equations. For all distances greater than the burst height (1480 ft), the values observed at an altitude of 100 ft were used.

3.6 PRECURSOR WAVE AND THERMAL EFFECTS

The excellent pressure-time records obtained by Project 6.1 (see WT-602) indicated conclusively the existence of a precursor wave over the land area, whereas gauges placed over the water detected a standard picture-book-type shock wave. Palm trees on an island in the foreground of the smoke-trail photographs completely obscured GZ and the island where the precursor was detected. No precursor was observed over the water surface, which was clearly

*Theories posed by G. I. Taylor, J. G. Kirkwood and S. R. Brinkley, F. B. Porzel, and others are in essential agreement with regard to the value of the exponent in this relation.

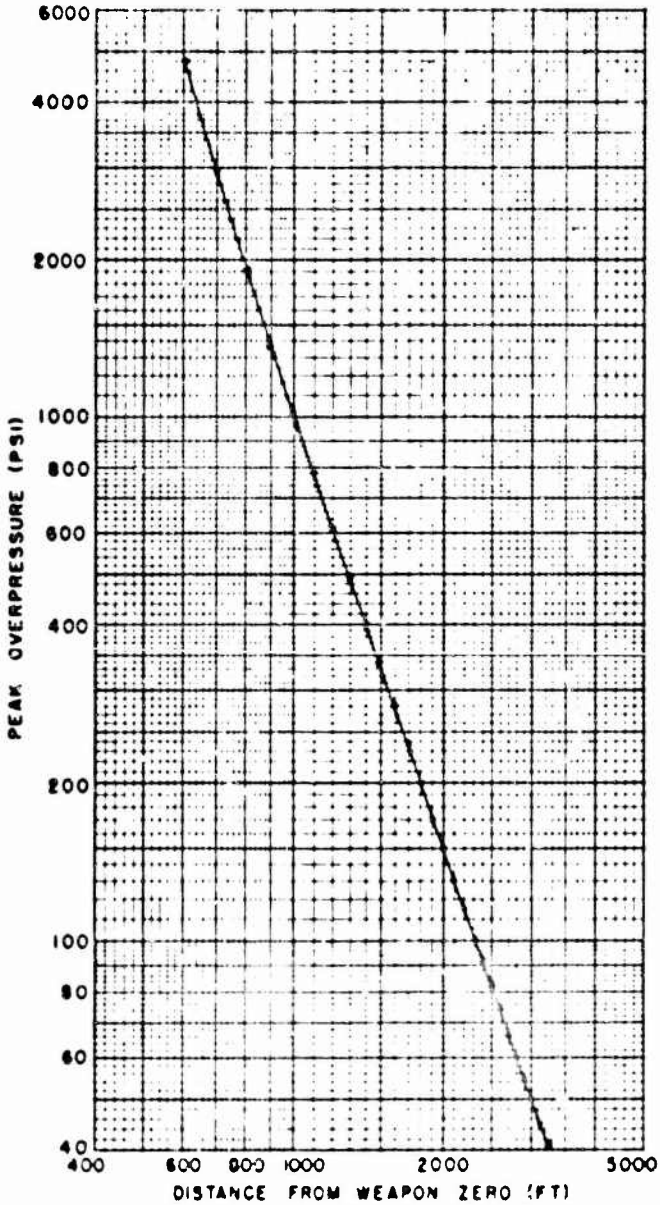

Fig. 3.4 — Peak overpressure vs distance from weapon zero.

visible in the films. This serves to confirm the gauge results over water. No thermal effects of any kind were observed in these photographs.

3.7 ACCURACY OF RESULTS

3.7.1 Sources of Error

The possible sources of error and the procedures for calculating their magnitudes are discussed in detail in reference 3. Each of the seven major sources of error listed below were given due consideration:

1. Timing calibration.
2. Static- and dynamic-resolution uncertainties associated with film measurements under ideal conditions.
3. Scaling distance on film.
4. Foreshortening of the image in the plane of measurement.
5. Meteorological data.
6. Curve fitting.
7. The variation of γ.

3.7.2 Timing Accuracy

The small number of timing marks which were placed on the film at a rate of 1.96 cps made it difficult to establish quantitatively the uncertainty in the time resolution. It was impossible to determine directly whether the film speed was constant over the entire region of interest. The average film speed was measured wherever possible. In the region of interest and the regions immediately beyond, the film speed was found to be the same. The first six frames of the record (film 16293) included the fireball and early transition regions, in which exceptionally accurate radial distances could be measured. When these were compared with the fireball growth measurements of EG&G, for which timing was highly accurate, it was found that the agreement was excellent. This is shown in Fig. 3.2. As a result the time per frame was established accurately over this region to within ±0.000150 sec per frame. It was assumed that the film rate was constant and that the time per frame used in the fireball region was valid throughout the entire period of interest. In the subsequent analysis the resulting data indicated that the film speed was constant by the more or less random distribution about the fitted arrival-time curve of Fig. 3.1. In addition, if the momentum of the film and the film drive is considered, it seems unlikely that there would be a significant variation in speed within 0.7 sec. The assumption of constant frame rate is thus considered reasonable.

3.7.3 Distance Accuracy

The accuracy in scaling distance is dependent on the measurements of the focal length of the lens and the distance from the camera to the object plane. The uncertainty in these measurements is known to be less than 0.1 per cent. After the center of burst is located on the film in any given early frame, its position is determined in the later frames by fixing its position with respect to the film sprocket holes. Assuming the camera to be operating normally, the variation of the position of the sprocket holes with respect to a given frame has been measured to be less than 1 per cent. For the film used to obtain the data, this amounts to an uncertainty of ±0.5 ft in the object plane. The maximum spatial static-resolution uncertainty was found to be ±6 ft. The maximum dynamic-resolution uncertainty falls within this limit. The foreshortening effect becomes increasingly important with increase in the shock-wave growth. It varies in a fixed manner over the range considered from 0.1 to 1.5 per cent of the radial distance measured. Corrections were calculated and applied for each distance.

As a result of these considerations an average figure of accuracy of ±2.5 ft is assigned to distance measurements in the free-air region.

[redacted]

3.7 4 Accuracy of Pressure-Distance Results

The errors in individual time and distance measurements are not carried over directly into the pressure calculations. These errors are substantially reduced by fitting the data with a curve by the method of least squares.[3] On the other hand, errors in P_0C_0 are carried over directly into pressure calculations. It is estimated that the error in these data is of the order of 1 per cent.

The error in the calculated pressures based on the derivatives of the fitted arrival-time curves and the atmospheric measurements mentioned above are considered to be accurate to 2.5 per cent at the 50-psi pressure level and increasingly more accurate at the higher levels.

REFERENCES

1. J. O. Hirschfelder and C. F. Curtiss, Thermodynamic Properties of Air, Vol. II, University of Wisconsin (NRL), Dec. 21, 1948.
2. C. J. Aronson, J. F. Moulton, Jr., et al., Free Air and Ground Level Pressure Measurements, Tumbler-Snapper Projects 1.3 and 1.5 Report, WT-513.
3. J. F. Moulton, Jr., and B. T. Simonds, Peak Pressure vs Distance in the Free-air and Mach Regions Using Smoke-rocket Photography, Greenhouse Report, Annex 1.6, Part II, Sec. 1, WT-54.

[redacted]

CHAPTER 4

ANALYSIS AND DISCUSSION OF RESULTS

In order to compare the results obtained on King Shot with those obtained on previous tests, it is necessary to reduce the data in some consistent manner such that one variable is common to both sets of data. On Operation Tumbler[1] the Sachs method[2-4] was used to reduce the data to standard sea-level atmospheric conditions, namely, 14.7 psi pressure and 293°K (20°C) temperature. In addition, the data were reduced further by applying the cube law for the charge weight. King Shot data have been treated similarly. When the data are reduced to the equivalent of 1 kt(RC) (radiochemical kilotonnage) at sea-level conditions, they are termed "A-scaled." This term will be used frequently in the following discussion.

4.1 SCALING FACTORS AND DATA REDUCTION

The scaling factors used to reduce the original results contained in Chap. 3 are given in Table 4.1. The arrival-time data and pressure-distance results have been A-scaled. Also, the pressure-distance results have been reduced to sea level. The reduced results have been compared with those of previous tests (1) to determine similarity of results, which is actually a test of the scaling laws, (2) to determine the yield in terms of radiochemical kilotonnage, and (3) to determine the TNT blast efficiency.

Table 4.1 — MISCELLANEOUS DATA AND SCALING FACTORS

Assigned ground zero (AGZ)	N 108,150 E 124,130
Actual ground zero (GZ)	N 108,450 ± 10 E 123,650 ± 20
Burst height (h), ft	1480 ± 20
Temperature at burst height (T_s), °C	25.4
Radiochemical yield (W_{RC}), kt(RC)	541 ± 30
Pressure at burst height before shot (P_s), psi	13.96
Factor to multiply pressures to correct to sea level ($S_p = 14.7/P_s$)	1.053
Factor to multiply distance to correct to sea level [$S_d = (P_s/14.7)^{1/3}$]	0.9829
Factor* to multiply distance to reduce to 1 kt(RC) at sea level [$S_d = (P_s/14.7W_{RC})^{1/3}$]	0.1206
Factor* to multiply time to reduce to 1 kt(RC) at sea level {$S_t = [(T_s + 273)/293]^{1/2} S_d$}	0.1217
A-scaled burst height (hS_d), ft	178 ± 2.4

*A-scaled factors.

4.2 YIELD OF KING SHOT

Before the results can be reduced, a reasonably accurate value of the yield (or radiochemical kilotonnage equivalent) must be determined. A tentative value for the yield was published by Ogle and Lofland[6] as 550 ± 50 kt. An independent determination based on the free air pressure-distance results given in Chap. 3 was made as follows:

1. Values of peak shock overpressure were taken from Table 3.3 and reduced to sea level by using the appropriate scaling factor.

2. These reduced pressures were located on the A-scaled pressure-distance Tumbler composite (Fig. 4.12 of reference 1), and the corresponding Tumbler distances were noted.

3. The ratios of these distances to the unreduced distances of King Shot given in Table 3.3 were determined and averaged over the entire free-air region.

4. The average value obtained for the ratio of the distances was 0.1206 ± 0.0023. Equating this value to the A-scaled factor $(P_0 / 14.7)(W_{RC})^{\frac{1}{3}}$ and using P_0 = 13.96 psi, the value for W_{RC} was found to be 541 ± 30 kt(RC). This value (541 kt) has been used throughout the following scaling procedures.

4.3 COMPARISON OF KING SHOT DATA WITH TUMBLER COMPOSITES

4.3.1 Arrival-time Data

The fireball and free-air A-scaled arrival-time data are given in Table 4.2. The free-air data are plotted with the A-scaled Tumbler composite arrival-time curve in Fig. 4.1. The data used in formulating the Tumbler composite curve and the equations representing it are given in Tables 4.5 to 4.8 and in Sec. 4.2.1 of reference 1.

The scale of Fig. 4.1, which includes only a small portion of the Tumbler composite curve, has been greatly enlarged to show the deviation of the King Shot data which fall within the limits of maximum uncertainty of the composite curve. The maximum uncertainty in the A-scaled composite curve is primarily governed by the values assigned to the radiochemical kilotonnages and secondarily by the compound errors in the time and space calibrations. The maximum uncertainty of all A-scaled Tumbler arrival-time data brought about by both primary and secondary causes was of the order of 2 per cent. The uncertainty in the King Shot data is of the same order.

Only on Tumbler Shots 3 and 4 were sufficient fireball data obtained with which the data of King Shot could be compared. This comparison is shown graphically in Fig. 4.2, where good agreement is indicated.

4.3.2 Peak-overpressure-Distance Data

The A-scaled pressure-distance results are given in Table 4.3 and are shown graphically in Fig. 4.3. The A-scaled Tumbler composite pressure-distance curve is included for comparison. The data used in the formulation of the Tumbler composite curve can be found in Tables 4.11 to 4.14 of reference 1.

On the average, the A-scaled King pressure-distance results agree with the Tumbler composite to within 2.0 per cent. At the extremes of the pressure range measured, however, the King data are low by approximately 8 per cent. Figure 4.3 represents the best possible overall fit with the Tumbler composite and provides the basis for the yield calculation of Sec. 4.2.

4.4 TNT BLAST EFFICIENCY

By fitting TNT pressure-distance data to data from King Shot, a value for the TNT efficiency of the nuclear weapon can be determined. The procedure used is as follows:

1. The free-air pressure-distance data for the nuclear explosion found in Table 3.3 were corrected to sea level (Table 4.3) and are plotted in Fig. 4.4.

Table 4.2 — A-SCALED ARRIVAL-TIME DATA

Distance from weapon zero, A-scaled, ft	Arrival time, A-scaled, sec	Distance from weapon zero, A-scaled, ft	Arrival time, A-scaled, sec
70.1	0.00138	288.1	0.04429
91.8	0.00281	291.7	0.04572
108.3	0.00424	294.6	0.04715
120.6	0.00567	299.8	0.04858
132.0	0.00710	304.3	0.05001
141.8	0.00853	307.5	0.05144
150.9	0.00996	311.3	0.05287
159.2	0.01139	314.9	0.05430
...	...	318.8	0.05573
177.2	0.01425	323.4	0.05716
184.3	0.01568	325.5	0.05859
190.4	0.01711	329.6	0.06002
197.0	0.01854	331.6	0.06145
202.7	0.01997	336.6	0.06288
210.3	0.02140	338.2	0.06431
217.0	0.02283	343.2	0.06574
223.2	0.02426	345.7	0.06717
226.1	0.02570	349.7	0.06860
231.5	0.02713	352.3	0.07003
236.3	0.02856	354.8	0.07146
244.0	0.02999	358.8	0.07289
246.8	0.03142	362.2	0.07433
252.0	0.03285	366.3	0.07576
257.8	0.03428	368.8	0.07719
263.3	0.03571	373.0	0.07862
265.8	0.03714	375.3	0.08005
270.7	0.03857	379.3	0.08148
273.5	0.04000	381.9	0.08291
279.3	0.04143	...	...
282.9	0.04286	387.4	0.08578
		390.8	0.08721

2. The theoretical A-scaled TNT pressure-distance data presented in Table 4.4 and shown in Fig. 4.5 are based on information published by Kirkwood and Brinkley[1] and Hartmann.[2] For equivalent pressures the corresponding distances were read from the curves of Figs. 4.4 and 4.5. The ratio of the nuclear distance to the TNT distance for each pressure level is equal to the cube root of the TNT kilotonnage [kt(TNT)] equivalent at that pressure.

3. The TNT efficiency for each pressure level was determined by cubing the distance ratio and dividing by the radiochemical yield of the nuclear weapon. The average efficiency was taken over a given pressure range, the upper limit of which is of the order of 200 psi, because for pressures higher than this the slope of the TNT pressure-distance curve falls off rapidly as compared to that for a nuclear explosion (see Fig. 4.5).

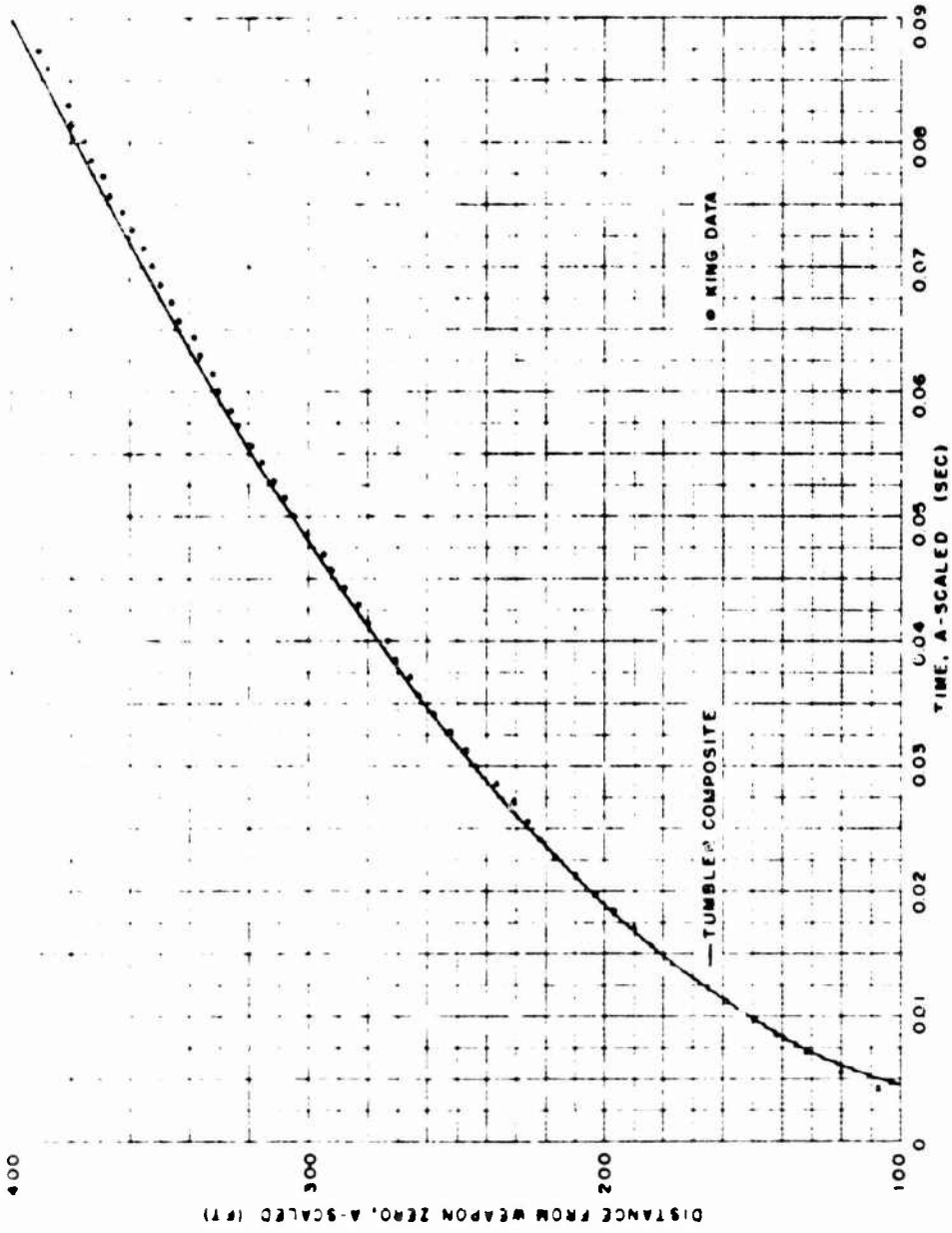

Fig. 4.1—A-scaled arrival-time data compared with Tumbler composite.

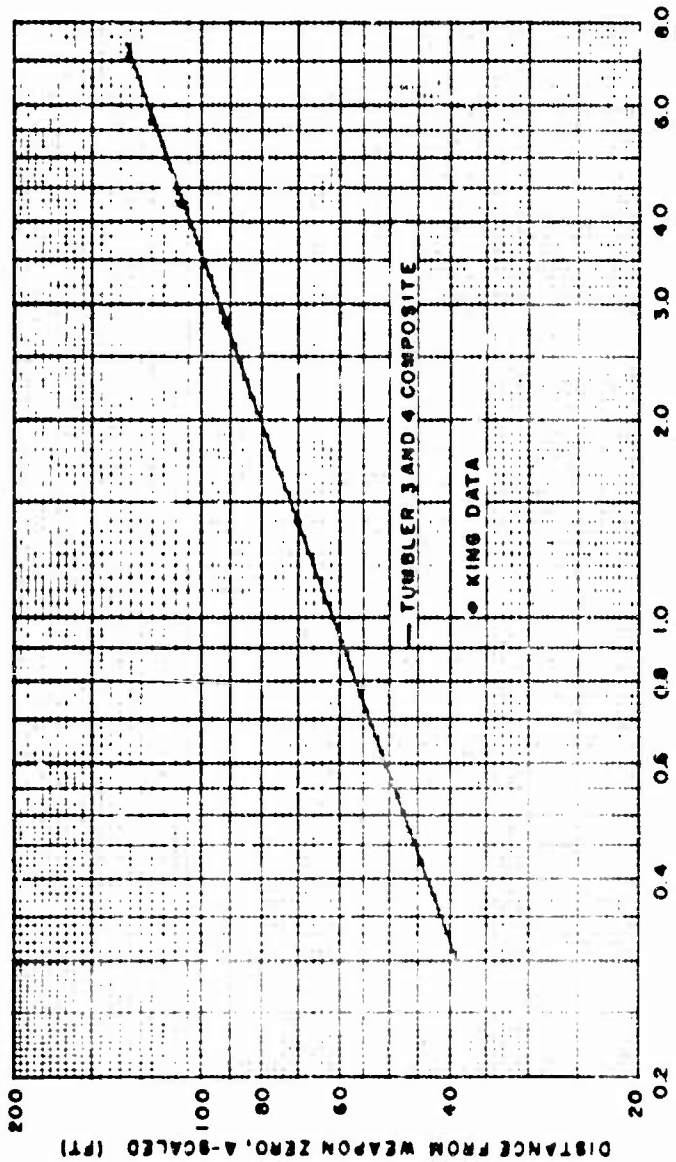

Fig. 4.2 — A-scaled fireball growth compared with Tumbler 3 and 4 composite.

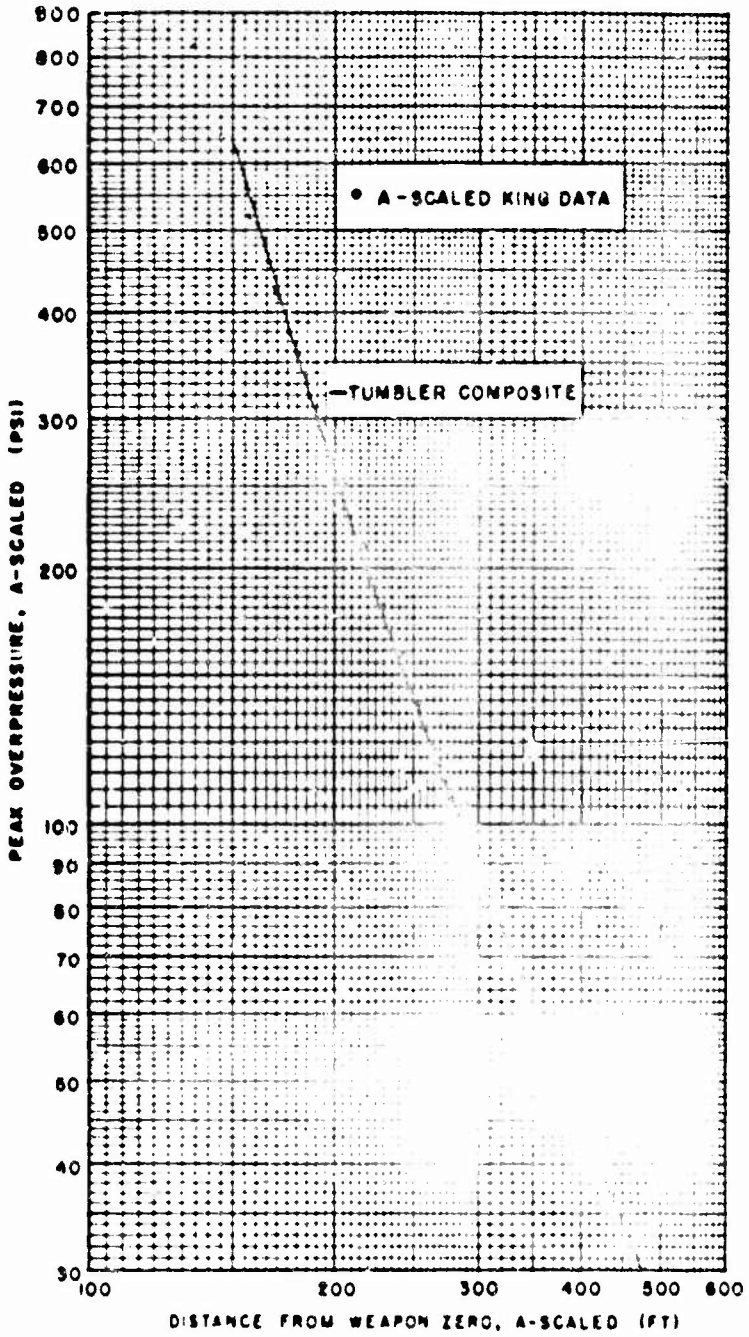

Fig. 4.3 — A-scaled pressure-distance data compared with Tumbler composite.

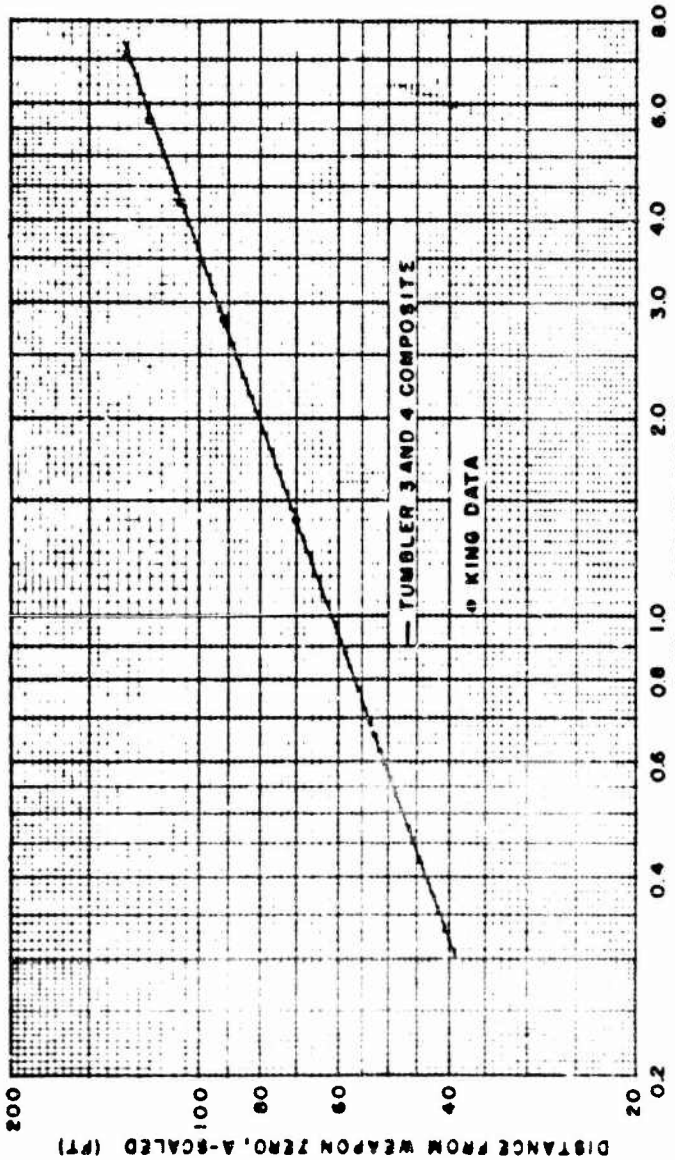

Fig. 4.2 — A-scaled fireball growth compared with Tumbler 3 and 4 composite.

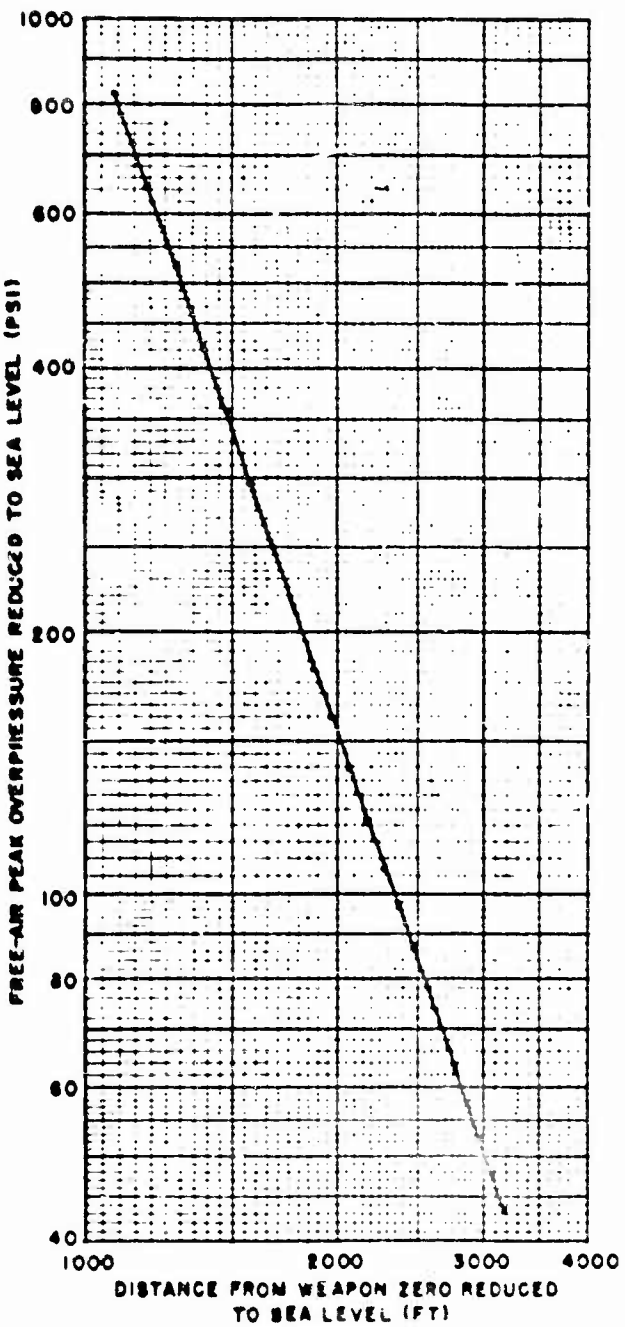

Fig. 4.4—Free-air peak overpressure vs distance from weapon zero, reduced to sea level

Table 4.3 — SCALED PEAK-OVERPRESSURE-DISTANCE DATA

Distance from weapon zero, ft	Distance from weapon zero, reduced to sea level, ft	Distance from weapon zero, A-scaled, ft	Peak overpressure, reduced to sea level, psi
600	590	72	5086
700	688	84	3118
800	788	98	2024
900	885	108	1454
1000	983	121	1070
1100	1081	133	823
1200	1179	146	645
1300	1278	157	522
1400	1376	169	426
1500	1474	181	359
1600	1573	193	298
1700	1671	205	251
1800	1769	217	214
1900	1868	229	181
2000	1966	241	159
2100	2064	253	139
2200	2162	265	122
2300	2261	277	107
2400	2359	289	97.0
2500	2457	302	87.0
2600	2558	314	78.6
2700	2654	328	70.9
2800	2752	338	63.2
2900	2850	350	57.7
3000	2949	362	52.3
3100	3047	374	47.7
3200	3145	388	43.2

4. The average value for the TNT efficiency, when multiplied by the radiochemical yield of the nuclear weapon, gives a value for the yield in terms of TNT kilotonnage. Use of this value in the King scaling operation produced the results shown in Fig. 4.5 in which the fit to the TNT data is illustrated.

Following this outline, the average TNT efficiency of King Shot was found to be 38.8 ± 2.0 per cent which corresponds to a yield of 209.8 kt(TNT) over the pressure range of 200 to 50 psi.

The percentage TNT efficiency as obtained above is lower than the Tumbler composite average of 42.1 per cent within the 300- to 50-psi pressure range. This is due chiefly to the fall-off of pressure at the lower end of the pressure range measured. It should be stressed again[1,3] that the value of TNT efficiency is very sensitive to small differences in the distances at which equivalent pressures are determined from one shot to the next. Because of the cube law that is brought into the calculations, these small differences are significantly magnified. Caution must be exercised when judging different sets of data on this basis.

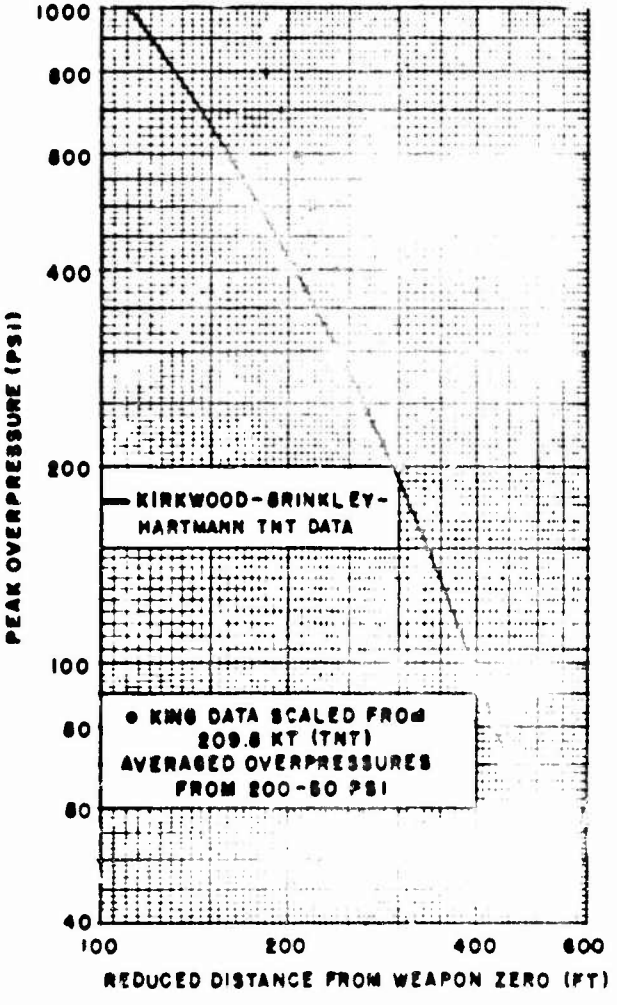

Fig. 4.8 — Free-air peak overpressure vs distance from weapon zero, reduced to 1 kt of TNT at sea level

Table 4.4 — COMPARISON OF KING SHOT DATA AND TNT DATA

Peak overpressure, psi	Radius for 1 kt of TNT at sea level, ft	Distance from weapon zero, reduced to sea level, ft	TNT equivalent of King, kt(TNT)	TNT efficiency of King, % $\left[\frac{\text{kt(TNT)} \times 100}{\text{kt(KC)}}\right]$	Distance from weapon zero, reduced to 1 kt(TNT) at sea level, ft*
800	132				184
700	145				194
600	160				205
500	179				218
400	204				237
300	241				264
200	295	1815	232.8	43.0	306
150	334	2015	219.5	40.6	339
100	393	2340	211.1	39.0	394
90	410	2435	209.5	38.7	410
80	430	2540	206.0	38.1	428
70	455	2670	202.0	37.3	449
60	480	2810	200.6	37.1	473
50	515	2995	196.7	36.4	504
			Av. 209.8 ± 10.7	38.8 ± 2.0	

*Values scaled on the basis of 209.8 kt(TNT).

REFERENCES

1. C. J. Aroneon, J. F. Moulton, Jr., et al., Free Air and Ground Level Pressure Measurements, Tumbler-Snapper Projects 1.3 and 1.5 Report, WT-513.
2. R. G. Sachs, The Dependence of Blast on Ambient Pressure and Temperature, BRL Report 466, May 15, 1944.
3. Army, Navy, and Air Force (JCS), TM 23-200/OPNAV-P-36-0010O/AFOAT 385.2, Supplement No. 1, Feb. 8, 1952.
4. H. H. M. Pike and J. H. Bird, The Reduction in Blast from Bare Chargee at High Altitudes, Armament Research Establishment Report 3/50, April 1950.
5. G. K. Hartmann, The Effect of Ambient Conditions on Air Blast, NavOrd Report 2482, June 20, 1952.
6. W. E. Ogle and J. H. Lofland, Cureory Report, Operation Ivy, Ref. Sym. J-16025, Dec. 1, 1952.
7. J. G. Kirkwood and S. R. Brinkley, Theoretical Blast Wave Curves for Cast TNT, OSRD Report 5481, August 1945.
8. J. F. Moulton, Jr., E. R. Walthall, and P. Hanlon, Peak Pressure ve Distance in Free Air Using Smoke Rocket Photography, Buster-Jangle Project 1.3b Report, WT-*89.

CHAPTER 5

CONCLUSIONS AND RECOMMENDATIONS

5.1 INSTRUMENTATION

The photographic results were good despite the facts that one camera failed to operate, that poor atmospheric conditions existed, and that timing marks were applied at a low rate. Timing signal relays and a-c power, housed in a new and very much cheaper shelter, worked properly, and all 19 rockets fired as planned. The fan-type grid, used because of the extreme space limitations imposed, proved to be very satisfactory. Compared to the vertical-line grid used on previous tests, three disadvantages were noted.

1. More rockets must be fired in order to achieve equivalent space coverage.
2. The rocket battery must be reasonably compact, which makes the loading operation more hazardous.
3. The probability of a trail coinciding with a radial line from the burst is increased. This is undesirable because the light refracted from such a trail cannot be readily detected.

As a result, it is recommended that the fan grid be used only if necessary.

5.2 DATA ANALYSIS

The use of IBM equipment decreased the time required to fit an analytical expression to the measured arrival-time data by 85 per cent. Identical results were obtained using both the new and the old methods; thus complete confidence can be placed in all the results, old and new alike. The average deviation of the data points from the fitted curve was less than 1 per cent in distance or time.

5.3 RESULTS

Arrival-time data were obtained throughout the first 0.7 sec, during which time the shock wave traveled out to approximately 3250 ft. Based on these data the following results were obtained for King Shot:

1. The yield of 541 ± 30 kt(RC) determined from the comparison of King results with Tumbler composite free-air pressure results is in good agreement with the value of 550 ± 50 kt(RC) given by Ogle and Lofland.[1] On this basis the range over which the scaling laws for free air can be used is extended to 550 kt(RC).

2. The TNT blast efficiency of King was of the same order as that of the Tumbler average, 38.8 and 42.1 per cent, respectively, in the pressure range of 300 to 50 psi. It is interesting to note that, as the kilotonnage increases, the TNT efficiency apparently decreases slightly (see reference 2 for comparison).

3. In the fireball region

$$R = 3302.3t^{0.380} \qquad R \leq 900 \text{ ft} \tag{5.1}$$
$$P \propto R^{-3.33}$$

whereas in the free-air region

$$t = 0.00141\left(R - \int_{R_0}^{R} \frac{5056.6^{1.6}}{5056.6^{1.6} + R^{1.6}}\, dR\right) - 0.6236 \qquad 900 \text{ ft} \leq R \leq 3250 \text{ ft} \tag{5.2}$$

where R is the radial distance from weapon zero in feet, t is the time in seconds, and P is the peak shock overpressure in pounds per square inch.

5.4 THERMAL EFFECTS

The precursor wave detected by the pressure-time gauges of Project 6.1 over the island of Runit could not be observed in the Project 6.13 films because the view of the island was obstructed by palm trees on an island in the foreground, and the camera location was poor in this respect. This situation was not remedied before the test because of insufficient time and man power. In the event of a similar test in the future, every effort should be made to assure an unobstructed view of GZ.

The films did not show a precursor wave over the water, although the view was unobstructed. This confirms the records produced by the gauges placed over the water by Project 6.1. These records showed that the shock wave had a fast rise time and decayed in the manner expected (see Ivy Project 6.1 report, WT-602).

No additional conclusive information was obtained to explain the deviation of Greenhouse free-air pressure-distance results from the Tumbler composite. There is only one thought concerning this problem wherein the King Shot results might indicate a solution. On the basis of relative energy incident at the ground, Greenhouse Easy was more than twice as effective as King; yet a precursor wave, believed to be formed as the result of the existence of a thermal layer,[3-4] was observed on King Shot. It is thus possible to conceive that the atmospheric heating associated with a thermal layer on Greenhouse was so intense that the shock wave in free air traveled much faster than it would in an unheated atmosphere. Since temperature measurements observed just prior to the burst on Greenhouse were used to compute the sonic velocity (which is used in the pressure calculations, Eq. 1.5), it is also conceivable that the values used were significantly low. This would explain the high pressures obtained at Greenhouse as compared with those from Tumbler, at least in part. The proximity of the ground and other arguments proposed in references 2 to 4 may also have contributed.

REFERENCES

1. W. E. Ogle and J. H. Lofland, Cursory Report, Operation Ivy, Ref. Sym. J-16025, Dec. 1, 1952.
2. C. J. Aronson, J. F. Moulton, Jr., et al., Free Air and Ground Level Pressure Measurements, Tumbler-Snapper Projects 1.3 and 1.5 Report, WT-513.
3. F. B. Porzel, Height of Burst for Atomic Bombs, Preliminary Draft of Report LA-1406, March 1952.
4. C. J. Aronson, J. F. Moulton, Jr., G. K. Hartmann, and J. D. McClendon, NOL Reports Presented at the Tumbler Symposium, U. S. Naval Ordnance Laboratory Report NavOrd 2801, March 1953.

APPENDIX

THE METHOD OF REDUCING THE DATA

By T. S. Walton

A.1 NATURE OF THE DATA

The experimental data consist in a large number of pairs of position and time measurements obtained from a high-speed motion-picture film of the shock wave from an explosion. The problem involved in reducing the data is basically that of finding a mathematical function which effectively correlates these observed values of position and time, so that the velocity of the shock front can be determined from the derivative of the function.

Some method of fitting the data which is based on the principle of least squares seems appropriate because the measurements are not exact but contain presumably random errors from many sources. The shock wave itself may not be propagated with perfect regularity because of the slight inhomogeneity of the atmosphere, and aside from this there are numerous errors introduced by the measuring equipment (for example, fluctuations in the speed of the camera motor and uncertainty in the location of the shock front due to the optical resolution of the lens system or the grain size of the film).

Prior to the completion of the analysis, it could not be ascertained whether the dispersion of the data was primarily the result of errors in the position or the time; so attempts were made to fit the observations both ways. In order to keep the analysis simple and minimize the amount of computation, polynomials in the time and in the distance were first tried and then later the ratio of two simple polynomials. However, these were generally unsatisfactory because they would fit only limited stretches of data. The junction points between successive curves were not smooth and showed very abrupt changes in slope.

The entire range of observations could have been approximated to any desired degree by introducing many more arbitrary parameters; but in such a case the approximating function would have too much "flexibility," and its derivative could oscillate wildly throughout the range of data points, leading to meaningless results.

A.2 THEORETICAL BASIS FOR THE ANALYSIS

The limited success achieved with arbitrary polynomials indicated that a theoretical basis for selecting an approximating function should be sought. It seemed desirable to find a form of function which corresponds as nearly as possible with the actual physical behavior of an explosion and also one in which the arbitrary parameters represent degrees of freedom having physical counterparts. The reliability of the fit could then be checked not only by observing the

[redacted]

trend of the residuals but also by comparing the a posteriori values of the parameters with reasonable a priori estimates of them.

A simplified approach to the problem is to treat the air surrounding the blast as a homogeneous medium of infinite extent obeying the equation of state of a perfect gas. To idealize the problem further, it is assumed that all the energy is suddenly released at a point within the medium (as heat energy available for performing work on the air but none being radiated). Then an attempt is made to deduce from the theoretical equations of gas dynamics the law which describes the motion of the shock wave and the manner in which it depends on the five parameters involved; namely, the original density, temperature, and specific heat ratio of the air and the total energy and time of inception of the blast.

A search of the literature revealed several noteworthy articles dealing with this problem. The basic theory was first developed in 1941 by Taylor,[1] the end result being

$$t - c = \left(\frac{K\rho}{E}\right)^{0.5} R^{2.5} \tag{A.1}$$

$$\frac{1}{U} = \frac{dt}{dR} = 2.5 \left(\frac{K\rho}{E}\right)^{0.5} R^{1.5} \tag{A.2}$$

where R = radius of the shock front
U = velocity of the shock front
t = time of arrival of the shock at R
c = time at which the blast began
E = total energy instantaneously released
K = a parameter depending on the specific heat ratio
ρ = original density of the air

The only additional assumption implicit in Taylor's solution is the strong shock condition, i.e., that the Rankine-Hugoniot relations assume their asymptotic forms corresponding to an infinite pressure ratio across the shock front. This assumption is correct as long as the Mach number of the shock is quite large, but it is clearly wrong in the limit as R increases indefinitely; for according to Eq. A.2 the velocity of the shock will ultimately drop to zero (rather than approach the velocity of sound, as it must). Taylor's formula is correct for large radii only when the temperature of the medium into which the shock expands is at absolute zero, so that both the pressure and the velocity of sound can be zero outside while the density remains finite.

Some progress toward removing this shortcoming in Taylor's solution has recently been made by Newton,[2] who modifies some of the flow assumptions to allow for the required behavior at both large and small radii. Newton shows that his equations do not violate any physical principles, but he is unable to obtain a complete solution because of the great complexity of the equations. However, he does find limiting solutions for both small and large radii. The result as R approaches zero agrees with that given by Taylor, while for large radii he finds that the velocity of the shock wave exceeds that of a sound wave by an amount which falls off as $1/R^{1.5}$.*

* This decay law for the excess velocity of spherical shock waves is somewhat at variance with the results of Brinkley and Kirkwood[3] and Whitham.[4] They obtain the formula $1 \; R \; [\log (R \; R_0)]^{0.5}$, where R_0 is some suitable constant. However, in each case their conclusions are arrived at on the assumption that at sufficiently great distances the shock wave becomes substantially an acoustic wave and that the flow across the shock front can then be considered isentropic. By contrast, Newton uses the exact Rankine-Hugoniot relations, and the change in entropy although seemingly negligible, may be the crux of the matter.

[redacted]

Newton's result immediately suggests a simple type of algebraic function which might be used to approximate the velocity of the shock for all radii, namely,

$$U = a\left[1 + \left(\frac{b}{R}\right)^{1.5}\right] \tag{A.3}$$

where a is the velocity of an acoustic wave in the region ahead of the shock and b is a scale parameter which depends on the initial density and temperature of the air and the amount of energy released. If this relation is assumed to be

$$b^3 = 0.16\,\frac{E}{K\rho a^2} \tag{A.4}$$

then Eq. A.3 can be written

$$U = a + \frac{0.4(E/K\rho)^{0.5}}{R^{1.5}} \tag{A.5}$$

and, if a is neglected, this reduces to Eq. A.2. Thus Taylor's formula for the velocity has merely been augmented by the amount a to account for the finite velocity of propagation of the wave as R approaches infinity, and this is compatible with his solution as R approaches zero since in that case the second term on the right side of Eq. A.5 becomes indefinitely large and the added contribution of the first term is then insignificant.

If reasonable agreement with a set of experimental data can be obtained by adjusting the parameters a and b in Eq. A.3, this quasi-theoretical formula can be substantiated. In order to carry out an actual fit, it is necessary to determine the mathematical relation between time and distance which this formula implies. The time of arrival of the shock at the point R is

$$t = c + \int_0^R \frac{1}{U}\,dR \tag{A.6}$$

Substituting the expression (Eq. A.3) for U,

$$t = c + \frac{1}{a}\int_0^R \left[1 - \frac{1}{1 + (R/b)^{1.5}}\right] dR \tag{A.7}$$

is obtained. For convenience in evaluating the integral, Eq. A.7 is written as follows:

$$t = c + \frac{R}{a} - \frac{b}{a}\int_0^s 2\left(\frac{s}{1+s^3}\right) ds \tag{A.8}$$

where $s = (R/b)^{0.5}$. Equation A.8 may be integrated to give

$$t = c + \frac{R}{a} - \frac{b}{3a}\left[2\sqrt{3}\,\arctan\frac{s\sqrt{3}}{2-s} - \log\frac{(s+1)^2}{s^2 - s + 1}\right] \tag{A.9}$$

The sum of the first two terms on the right side of Eq. A.9 corresponds to the time of arrival of an acoustic wave at the position R, and the last term accounts for the lead time of a spherical shock wave over an acoustic wave. It is interesting to note that the integral occurring in Eq. A.8 has an asymptotic value of 2.4184 when the upper limit of integration

[redacted]

approaches infinity. This can be interpreted by saying that a spherical shock wave will overtake an acoustic wave which previously emanated from the same point in space, provided that the latter did not have a head start exceeding 2.4184 (b/a) time units.*

Each of the parameters in Eq. A.9 has a physical interpretation, and this should facilitate the comparison of fitted data obtained from different tests. The quantity c is simply the time intercept, a is the asymptotic value of the velocity, and b is proportional to the physical dimensions of the blast, which vary as the cube root of the energy released. The well-known scaling laws for explosive phenomena may be applied to Eqs. A.3 and A.9. For example, the Mach number of the shock (U/a) depends only on the nondimensional ratio (R/b), and consequently the trajectory of the shock front will be similar for an explosion of any size in a given medium if the time and distance scales are both multiplied by a factor proportional to b.

Thus it is seen that the data may be presented in terms of any desired units of distance and time. The time values may also contain an additive constant, i.e., zero clock time need not correspond to the start of the blast. However, the radial distances must be referred to the true center of the explosion, although they may be scaled by an arbitrary factor.

A.3 COMPUTATIONAL PROCEDURE

In this section is given an outline of a procedure for determining the values of the parameters in the approximating function by the method of least squares. Although in principle the process of fitting a given set of data could be carried out by manual computation, it would be very laborious and time consuming; so it will be presumed that the routines described in the following are to be programed for automatic digital computing machines.

Let the symbol $f = f[a,b,c,R]$ stand for the mathematical function which approximates the measured time $t[R]$, the quantities in brackets indicating the functional relations involved. For convenience, Eq. A.7 is rewritten as

$$f = c + (x - y)\frac{b}{a} \tag{A.10}$$

where

$$x = \frac{R}{b} \qquad y = \int_0^x \frac{dx}{1 + x^{1.1}}$$

This permits the calculation to be carried out in terms of nondimensional quantities x and y. To simplify the analysis, it is assumed that the values of R are given exactly and that all the values of t have been corrupted by statistical errors of uniform dispersion. The validity of this assumption can be checked by a careful inspection of the final results of the computation. The residual error associated with the ith data point is defined as

$$e_i = f_i - t_i = (x_i - y_i)\frac{b}{a} + c - t_i \tag{A.11}$$

* By way of contrast, the decay law discussed in the preceding footnote gives a lead time proportional to the factor $\sqrt{\log (R/R_0)}$ which has no limit as R approaches infinity. This indicates that a spherical shock wave (regardless of how weak) would eventually overtake any acoustic wave regardless of how much earlier it has been emitted, a result contradictory to common sense.

[redacted]

[redacted]

and to make the problem definite it is supposed that, in accordance with the theory of probability, the "best" set of values for the parameters a, b, and c has been found when the sum of squares of all the residuals is a minimum. Now the residual equation (Eq. A.11) is seen to involve the parameters 1/a and c in a linear manner, but this is not true of b on account of the way in which x and y depend on b. Consequently the usual procedure for obtaining the normal equations for determining the best values of the parameters would lead to an intractable system of nonlinear equations (with no unique solution but an indefinite number of solutions, among which not more than one would be subject to physical interpretation).

To avoid this difficulty, the method of "differential corrections"[5] for iteratively improving an initially guessed-at set of values is used. The function f defined by Eq. A.10 can be expanded in a Taylor series about the point (a,b,c,R_i). Thus the change induced in f by small changes in a, b, and c may be expressed as

$$\Delta f = \left(\frac{\partial f}{\partial a}\right)\Delta a + \left(\frac{\partial f}{\partial b}\right)\Delta b + \left(\frac{\partial f}{\partial c}\right)\Delta c + \text{higher order terms} \tag{A.12}$$

Provided that the initial values are chosen sufficiently close to the desired solution, all terms beyond the first order may be neglected, and the residual associated with the ith point becomes

$$(f_i + \Delta f_i) - t_i = (f_i - t_i) + A_i\Delta a + B_i\Delta b + C_i\Delta c \tag{A.13}$$

where $A_i = (\partial f_i/\partial a)$ holding b, c, and R_i constant; $B_i = (\partial f_i/\partial b)$ holding a, c, and R_i constant; and $C_i = (\partial f_i/\partial c)$ holding a, b, and R_i constant.

The problem now reduces to finding the corrections which make the sum of squares of the new residuals a minimum. This leads to a system of three simultaneous linear equations in the unknowns Δa, Δb, and Δc, namely,

$$\begin{aligned}
(\Sigma A_i^2)\Delta a + (\Sigma A_iB_i)\Delta b + (\Sigma A_iC_i)\Delta c &= \Sigma A_i(t_i - f_i)\\
(\Sigma B_iA_i)\Delta a + (\Sigma B_i^2)\Delta b + (\Sigma B_iC_i)\Delta c &= \Sigma B_i(t_i - f_i)\\
(\Sigma C_iA_i)\Delta a + (\Sigma C_iB_i)\Delta b + (\Sigma C_i^2)\Delta c &= \Sigma C_i(t_i - f_i)
\end{aligned} \tag{A.14}$$

The solution of the system (Eq. A.14) gives the first-order corrections to be added to the initial values of a, b, and c. The results may be improved by repeating the process, using the "corrected" values in place of the original choices. However, this method will not always converge to the desired solution if the initial guesses are not accurate enough or if the dispersion of the data due to random errors is excessive.

An appropriate initial value for a is to use the velocity of sound corresponding to the prevailing atmospheric conditions at the time of the blast. The value of b might be estimated on the basis of the equivalent energy of the blast (if this were known) as indicated in Eq. A.4. Alternatively, the quantity $0.16/e^2b^3$ can be substituted for $K\rho/E$ in Taylor's solution for small R (Eq. A.1), the result being

$$(t-c)^2 = \frac{0.16R^3}{e^2b^3} \tag{A.15}$$

This can also be obtained by dropping the additive constant 1 in Eq. A.3 before carrying out the integration of $1/U$. For the ith data point, Eq. A.15 may be written

$$b = \left[\frac{0.16R_i^3}{e^2(t_i-c)^2}\right]^{\frac{1}{3}} \tag{A.16}$$

[redacted]

[redacted]

Equation A.16 can be used to estimate b provided that a pair of data values R_1 and t_1 are taken sufficiently near the origin of the blast that the Mach number of the shock at that point is large compared to unity. Obviously this procedure requires estimates of both a and c, whereas the procedure based on the equivalent energy of the blast does not require any knowledge of c. However, the origin of the time scale can usually be found from independent measurements.

Aside from the foregoing, no preliminary value is needed in the case of c since it enters the definition of f (Eq. A.10) in a completely linear manner, and it follows that the solution of the system of Eq. A.14 is independent of c. This is readily seen by examining the expressions used for calculating the values of A_i, B_i, and C_i. Thus, carrying out the partial differentiations of f with respect to a, b, and c as indicated following Eq. A.13,

$$\begin{aligned} A_i &= -\left(\frac{b}{a^3}\right)(x_i - y_i) \\ B_i &= \left(\frac{1}{a}\right)\left(\frac{x_i}{1 + x_i^{1.5}} - y_i\right) \\ C_i &= 1 \end{aligned} \tag{A.17}$$

The required values of the definite integral y can, of course, be obtained from tables of the inverse tangent and natural logarithmic functions as indicated in Eq. A.9. However, when the computations are to be carried out on an automatic digital computing machine, the entire procedure can be greatly expedited by evaluating y from an analytic continued fraction, namely,

$$\begin{aligned} y = \int_0^x \frac{dx}{1 + x^{1.5}} &= \int_0^s \frac{2s\,ds}{1 + s^3} \\ &= \cfrac{2s^3}{2 + \cfrac{4s^3}{5 + \cfrac{9s^3}{8 + \cfrac{25s^3}{11 + \cfrac{36s^3}{14 + \cfrac{64s^3}{17 + \cfrac{81s^3}{20 + \cdots}}}}}}} \end{aligned} \tag{A.18}$$

where $s^3 = x = R/b$. This is a special case (for the 1.5-power index) of a formula given by Wall.[6] A dozen or so terms of this continued fraction are sufficient to determine accurate values of the integral for arguments up to $s = 2$ (i.e., for radii not exceeding 4b), at which point the velocity of the shock has dropped to 1.125 times a. Although it is not likely to occur in practice, a greater range for the upper limit could be handled by employing more terms since the continued fraction (Eq. A.18) converges for all positive values of s.

A.4 CONCLUSION

The results obtained by fitting several sets of data to a formula of the type described indicate that Eq. A.9 is a good approximation to the trajectory of the shock from a strong explosion. The residuals for some of the most reliable data show a dispersion of about 2 msec in the time measurements over the entire range of data. However, they are not completely random but exhibit a number of positive and negative groupings. The period of this fluctuation does not appear to change with increasing radius but remains practically constant, which suggests that the oscillation is not inherent in the blast phenomenon but results instead from a deficiency in the meth-

[redacted]

[redacted]

od of measuring the time (for example, variations in camera speed). There is also some evidence that, if this periodic oscillation could be taken out of the time data, the remaining dispersion could be attributed to random errors of about 2 ft in the location of the shock front determined from each frame of film.

From a study of the data available at this time, it seems best to ascribe the inherent errors to the time measurements, and this leads to the simplest method of treatment. If it should ever prove desirable to assume that the times are given accurately and that errors are present in the positions only with a uniform dispersion, it would still be possible to employ the procedure described here. All that is necessary is to multiply each term in the residual equation (Eq. A.13) by a weighting factor proportional to the velocity, as given by Eq. A.3, so that, in forming the coefficients of the normal equation (Eq. A.14), the square of this factor would enter each product. This should be done with caution, however, since it will give very large weights to data near the beginning of the range. It is also clear that the approximate value of b must be known in advance in order to determine such a weighting factor, namely, $1 + (b/R_1)$.[1,6]

Finally, it was observed that the value obtained for a was quite sensitive to fluctuations in the data near the end of the record of observations. This is to be expected, of course, since a represents the asymptote of the velocity. An unusually large deviation near the end of the record or a gradual change in the speed of the camera would exert an exaggerated influence on the value obtained for a. Whenever a set of data encompasses a very limited range of radii, it is probably better to assign the velocity of sound permanently to a and to determine only b and c from the data. If it should be desired, the values of any of the parameters can be fixed in advance and only the remaining ones determined according to the least-squares criterion.

REFERENCES

1. G. I. Taylor, The Formation of a Blast Wave by a Very Intense Explosion, Proc. Roy. Soc. London, A201: 159-186 (1950).
2. R. G. Newton, A Progressing-Wave Approach to the Theory of Blast Shock, J. Appl. Mechanics, 19: 257-262 (1952).
3. S. R. Brinkley and J. G. Kirkwood, Theory of the Propagation of Shock Waves, Phys. Rev., 71: 606-611 (1947).
4. G. B. Whitham, The Propagation of Spherical Blast, Proc. Roy. Soc. London, A203: 571-581 (1950).
5. J. B. Scarborough, "Numerical Mathematical Analysis," Art. 115, p. 374, Johns Hopkins Press, Baltimore, 1930.
6. H. S. Wall, "Continued Fractions," p. 345, D. Van Nostrand Company, Inc., New York, 1948.

[redacted]

DATE: Oct 25 1995 18:13:51 TRIS INPUT REPORT PAGE: 156
EAB51ZR CYCLE IO: FM
CLASSIFICATION: UNCLASSIFIED

\01 AO-363573
\02 19110C.081100,190900
\03 U
\05 naval ordnance lab white oak md
\06 peak overpressure vs distance in free air,
\08 U
\10 Moulton,J. F. ,Jr.
Hanlon,P.
\11 19530300
\12 55
\18 AEC
ATOMIC ENERGY COMMISSION WASHINGTON DC
\19 WT-613
\20 U
\21 Report on Operation IVY, Project 6.13. (U)
\22 Approved fro public release;Oistribution unlimited.
\23 (•NUCLEAR EXPLOSIONS, PRESSURE)
\24 U
\25 ivy operation, king shot, precursors, RANGE(OISTANCE), SHOCK WAVES, BLAST, THERMAL PROPERTIES, VELOCITY, MATHEMATICAL ANALYSIS, EQUATIONS, EXPERIMENTAL OATA, GRAPHICS, TABLES(OATA), EXPLOSION EFFECTS, DETONATION WAVES, TEST METHODS, SEISMIC WAVES
\26 U
\27 At the request of the Height Burst Panel, Project 6.13 was organized to make measurements on King Shot, Operation Ivy, that would establish the peak shock overpressure in the blast wave as a function of distance from the burst in the freeair region. This information was required in particular to determine whether scaling laws could be used with existing data obtained on Operation Tumbler to predict free-air pressures from much larger weapons. Secondary cbjectives were to record and determine the magnitude of a precursor wave or other visibly observable thermal effects that might occur and to collect any additional information that might explain the departure of the free-air blast measurements obtained on Operation Greenhouse from the Operation Tumbler composite free-air pressure results. (The four free-air pressure-distance curves obtained on Operation Tumbler scaled very well over the entire pressure range measured. The composite result is considered to be highly reliable.) (Author)
\28 U
\29 2
\30 Peak overpressure vs distance in free air.
\32
\33 1
\35 250650
\36 1
\40 2405
\41 n
\49 951025 - (c-frd to u/dna-sstl ltr dtd 19 oct 95), & P'blc R'lse, E/4 to A1, per same ltr., signed by J.B. Wood, Chief, Tech Support.

Defense Nuclear Agency
6801 Telegraph Road
Alexandria, Virginia 22310-3398

SSTL

ERRATA

19 October 1995

MEMORANDUM FOR DEFENSE TECHNICAL INFORMATION CENTER
ATTENTION: OCD/Mr. Bill Bush

SUBJECT: Classification Review of AD-363573L

The Defense Nuclear Agency Security Office has reviewed and declassified the subject report (AD-363573L, WT-613).

Distribution statement "A" (**Approved for Public Release**) applies.

FOR THE DIRECTOR:

JOSEPHINE B. WOOD
Chief, Technical Support

15L. 20/8

ERRATA

26 Oct 95
Ltr & print to Ms Campbell
for Action

Defense Special Weapons Agency
6801 Telegraph Road
Alexandria, Virginia 22310-3398

JUN 11 1997

OPSSI

MEMORANDUM FOR DISTRIBUTION

SUBJECT: Declassification Review of Operation IVY Test Reports

The following 31 (WT) reports concerning the atmospheric nuclear tests conducted during Operation IVY in 1952 have been declassified and cleared for open publication/public release:

WT-602 through WT-607, WT-609 thru WT-618, WT-627 thru WT-631, WT-633, WT-635, WT-636, WT-639, WT-641 thru WT-644, WT-646, and WT-649.

An additional 2 WTs from IVY have been re-issued with deletions. They are:

WT-608, WT-647.

These reissued documents are identified with an "Ex" after the WT number. They are unclassified and approved for open publication.

This memorandum supersedes the Defense Nuclear Agency, ISTS memorandum same subject dated August 17, 1995 and may be cited as the authority to declassify copies of any of the reports listed in the first paragraph above.

RITA M. METRO
for Chief, Information Security